

Susceptibility factor RTP1 negatively regulates *Phytophthora parasitica* resistance via modulating UPR regulators bZIP60 and bZIP28

Xiaoyu Qiang ^{1,2}, Xingshao Liu ^{1,2}, Xiaoxue Wang ^{1,2}, Qing Zheng,^{2,3} Lijuan Kang,^{1,2} Xianxian Gao,^{1,2} Yushu Wei ^{1,2}, Wenjie Wu ^{1,2}, Hong Zhao,^{2,3} and Weixing Shan ^{1,2,*†}

1 College of Agronomy, Northwest A&F University, Yangling, Shaanxi 712100, China

2 State Key Laboratory of Crop Stress Biology for Arid Areas, Northwest A&F University, Yangling, Shaanxi 712100, China

3 College of Plant Protection, Northwest A&F University, Yangling, Shaanxi 712100, China

*Author for communication: wxshan@nwfau.edu.cn

†Senior author.

X.Q, X.L., and X.W. contributed equally to this work.

X.Q. and W.S. conceived and designed the research. X.Q., X.L., X.W., Q.Z., L.K., X.G., Y.W., and H.Z. performed the experiments. X.Q., X.L., X.W., X.G., Y.W., and W.W. analyzed data. X.Q. and W.S. wrote the article with help of all authors.

The author responsible for distribution of materials integral to the findings presented in this article in accordance with the policy described in the Instructions for Authors (<https://academic.oup.com/plphys/pages/general-instructions>) is: Weixing Shan (wxshan@nwfau.edu.cn).

Abstract

The unfolded protein response (UPR) is a conserved stress adaptive signaling pathway in eukaryotic organisms activated by the accumulation of misfolded proteins in the endoplasmic reticulum (ER). UPR can be elicited in the course of plant defense, playing important roles in plant–microbe interactions. The major signaling pathways of plant UPR rely on the transcriptional activity of activated forms of ER membrane-associated stress sensors bZIP60 and bZIP28, which are transcription factors that modulate expression of UPR genes. In this study, we report the plant susceptibility factor *Resistance to Phytophthora parasitica 1* (*RTP1*) is involved in ER stress sensing and *rtp1*-mediated resistance against *P. parasitica* is synergistically regulated with UPR, as demonstrated by the simultaneous strong induction of UPR and ER stress-associated immune genes in *Arabidopsis thaliana rtp1* mutant plants during the infection by *P. parasitica*. We further demonstrate RTP1 contributes to stabilization of the ER membrane-associated bZIP60 and bZIP28 through manipulating the bifunctional protein kinase/ribonuclease IRE1-mediated bZIP60 splicing activity and interacting with bZIP28. Consequently, we find *rtp1bzip60* and *rtp1bzip28* mutant plants exhibit compromised resistance accompanied with attenuated induction of ER stress-responsive immune genes and reduction of callose deposition in response to *P. parasitica* infection. Taken together, we demonstrate RTP1 may exert negative modulating roles in the activation of key UPR regulators bZIP60 and bZIP28, which are required for *rtp1*-mediated plant resistance to *P. parasitica*. This facilitates our understanding of the important roles of stress adaptive UPR and ER stress in plant immunity.

Introduction

To circumvent invasion by a plethora of pathogens, plants have evolved a two-layered innate immune system.

Perception of pathogen-associated molecular patterns (PAMPs) constitutes the first layer of plant innate immunity and is referred to as PAMP-triggered immunity (PTI). The

second layer is effector-triggered immunity that is often accompanied by hypersensitive response (HR; Jones and Dangl, 2006; Dodds and Rathjen, 2010). These innate immune systems often rely on basic cellular processes to defend pathogenic invasion, such as the endoplasmic reticulum (ER) quality control (ER-QC) system (Li et al., 2009) and hormone signaling (Tsuda et al., 2009). Thus, insights into the key regulators of these cellular processes during plant–pathogen interactions reveal orchestrating factors in plant immunity and defense mechanisms.

In eukaryotic cells, secreted and transmembrane proteins are translocated into the ER, where they are properly folded and modified through the sophisticated ER-QC system before being transported to their functional destination (Liu and Howell, 2010). Under abiotic or biotic stress, unfolded or misfolded proteins accumulate in the ER lumen, leading to the occurrence of ER stress. To release ER stress and restore ER homeostasis, ER membrane-associated stress sensors, such as the transcription factors (TFs) bZIP28 and bZIP60 subsequently activate the unfolded protein response (UPR; Liu et al., 2007; Iwata et al., 2008; Howell, 2013). The UPR comprises induction of ER chaperones and foldases (e.g. binding proteins, BiP), attenuation of protein translation and potentiation of protein secretion as well as degradation (Liu and Howell, 2010, 2016; Jäger et al., 2012; Kørner et al., 2015). In plants, there are at least two signaling pathways of UPR that are mediated either by inositol requiring enzyme 1 (IRE1)/bZIP60 or by bZIP28 (Kørner et al., 2015). IRE1 is a bifunctional protein kinase (PK)/ribonuclease (Deng et al., 2013). The activation of the IRE1-mediated unconventional splicing of mRNA is the most conserved UPR pathway in eukaryotes (Chen and Brandizzi, 2013; Ruberti et al., 2015). In plants, the sensor domain of IRE1 binds to the ER-luminal BiP and the full-length bZIP60 is anchored to the ER membrane under normal conditions. In response to ER stress, BiP dissociates from IRE1 to assist proper folding of the accumulated unfolded proteins (Iwata and Koizumi, 2005; Howell, 2013). The released IRE1 is dimerized to align its cytosolic kinase domain in such a way that they trans-autophosphorylate each other to activate further splicing of bZIP60 mRNA (Nagashima et al., 2011; Iwata and Koizumi, 2012; Mishiba et al., 2013). The spliced bZIP60 mRNA derived protein is transported into nucleus, which functions as TF to activate UPR genes (Deng et al., 2011; Humbert et al., 2012). In the other pathway of UPR, bZIP28 TF acts as ER stress sensor and is crucial to activate UPR (Iwata and Koizumi, 2012). Under normal conditions, the bZIP28 and cochaperone protein are anchored to the ER membrane by interacting with BiP (Williams et al., 2010; Li et al., 2017). In response to ER stress, BiP dissociates from bZIP28 and the released bZIP28 traffics to the Golgi and is proteolytically cleaved by site-1 (S1P) and site-2 proteases (S2P), which further translocates into the nucleus, where it functions to activate UPR genes (Liu and Howell, 2010; Srivastava et al., 2012; Iwata et al., 2017).

Increasing evidence demonstrates that proper ER function and UPR regulation play crucial roles in plant immunity. For instance, disturbance of ER-QC results in improper processing of the pattern-recognition receptor EFR and impairs plant immunity (Nekrasov et al., 2009; Saijo et al., 2009). Furthermore, the IRE1/bZIP60-mediated UPR pathway is of importance for inducing systemic-acquired resistance (SAR) against bacterial pathogens and abiotic stress tolerance (Moreno et al., 2012). Intriguingly, in rice (*Oryza sativa* L.), the underlying SAR-mediated priming effect depends on WRKY33, a gene that is known to be involved in salicylic acid (SA)-mediated defense in *A. thaliana* (Wakasa et al., 2014). Moreover, OsWRKY45 was reported to play a key role in SA-induced plant immunity and is induced by OsIRE1-mediated ER stress, indicating functional integration of plant immunity with ER stress signaling (Hayashi et al., 2012). SA is an important plant hormone, which regulates plant immunity, particularly upon infection by biotrophic pathogens (Glazebrook, 2005). As a master regulator of SA-dependent responses to pathogens, NPR1 was recently reported to interact with UPR TFs bZIP28 and bZIP60 in the nucleus and negatively regulates the activation of UPR independently from SA (Lai et al., 2018). Notably, the ER-localized FKBP15-2 protein is a direct target of *P. capsici* effector PcAvr3a12 and is a positive immune factor in regulating ER stress-mediated plant immunity (Fan et al., 2018).

During a compatible plant–pathogen interaction, there are key regulators which facilitate pathogen invasion into host plant, namely, susceptibility factors (Pavan et al., 2010; van Schie and Takken, 2014). They could either manipulate the plant target proteins which are recognized by pathogens or negatively regulate plant immune response to facilitate compatible plant–pathogen interaction. Because the loss-of-function or mutation of susceptibility genes enhances plant durable resistance and confers broad-spectrum resistance to host plant, they are potentially applied in molecular breeding for crop disease resistance. For instance, the natural variation in the promoter of *Bsr-d1*, which is a crucial regulator of rice blast disease resistance, improves plant resistance without obvious loss of rice yield and quality (Li et al., 2017). However, the molecular mechanisms of how ER-associated or ER-regulated processes participate in plant immunity mediated by susceptibility factors remain less understood.

Oomycetes, particularly *Phytophthora* species, cause serious crop diseases, such as potato late blight, and threaten the sustainable crop production worldwide (Fry, 2008). Because of the prominent variation of pathogen virulent genes and loss-of-function of genotype-specific plant resistant genes during evolution, understanding and utilization of novel factors that confer broad-spectrum and durable resistance have attracted great attention in the field of plant–oomycete interaction researches. *Phytophthora parasitica* is a typical hemibiotrophic oomycete pathogen, which has a wide range of hosts and seriously threatens agricultural

production (Meng et al., 2014). With the established compatible interaction system between *A. thaliana* and *P. parasitica* (Wang et al., 2011), the susceptibility factor *resistance to Phytophthora parasitica 1* (*RTP1*) was identified to render *A. thaliana* more resistant to infection by pathogens including *P. parasitica* (Pan et al., 2016). Further studies have demonstrated that *RTP1* encodes an ER membrane-localized protein and affects the transcription of SA-responsive gene *PR1* during the early infection stage (Pan et al., 2016). However, the mechanism of how *RTP1* negatively regulates plant resistance remains largely unknown.

In this study, we address the question whether *rtp1*-mediated plant resistance is synergistically regulated with ER stress signaling. We show that the loss of functional *RTP1* exhibits altered tolerance to ER stress induced by tunicamycin (TM), a well-established ER stress inducer. Simultaneously, it displays stronger induction of UPR and ER stress-associated immunity in response to early infection by *P. parasitica*. Our analyses further demonstrate that *RTP1* contributes to stabilization of the ER membrane-bound stress sensors bZIP60 and bZIP28 through manipulating the bifunctional protein kinase/ribonuclease IRE1-mediated bZIP60 splicing activity and interacting with bZIP28. On the basis of these results and the evidence of compromised resistance in *rtp1bzp60* and *rtp1bzp28* mutants shown in this work, we propose that *RTP1* functions as a negative regulator of the activation of bZIP60 and bZIP28 UPR TFs, which are required for *rtp1*-mediated plant resistance to *P. parasitica*. Together, this work identifies the susceptibility factor *RTP1* as a critical modulator of the plant UPR and facilitates to understand convergence of signaling decoding in UPR and plant immunity.

Results

RTP1 is involved in general ER stress and UPR regulation

According to a previous study, *RTP1* encodes an ER-localized protein that mediates plant susceptibility to *P. parasitica* (Pan et al., 2016). This finding prompted us to question whether *RTP1* is involved in ER stress and the subsequent UPR signaling pathway, which mediates the immune function of *RTP1* against *P. parasitica*. To test this, 5-d-old seedlings of *A. thaliana* wild-type (WT) Col-0 and *rtp1* mutant were treated with TM to induce ER stress by inhibiting N-linked glycosylation. Seedlings treated with dimethyl sulfoxide (DMSO) were used as controls. At 5 d post treatment, the fresh weight of the seedlings was measured. The results showed ~40% of reduction in fresh weight for the TM-treated WT Col-0 seedlings compared with that of the DMSO-treated seedlings. In contrast, TM treatment resulted in around 55% of biomass reduction in the *rtp1* mutants compared with control DMSO treatment (Figure 1A), suggesting that *rtp1* mutants seem hypersensitive to TM-induced ER stress.

To further examine whether *RTP1* is involved in ER stress, seedlings of WT Col-0 and *rtp1* mutant were initially grown on medium supplemented with TM, followed by 10 d of growth without TM. Thereafter, the recovery rate of seedlings was calculated as described (Moreno et al., 2012). Around 80% of WT Col-0 seedlings were rescued from TM treatment. In comparison, *rtp1* mutants exhibited distinct chlorosis and noticeable growth retardation, showing merely 20% of seedlings recovered. Notably, this reduced recovery rate was complemented in *RTP1*-OE transgenic lines, since in these lines ~85% of seedlings rescued from TM treatment (Figure 1B). *Arabidopsis thaliana* γ VPE had been documented to be involved in ER stress-mediated cell death and γ vpe mutants were shown insensitive to TM (Qiang et al., 2012). Expectedly, γ vpe mutants were less affected by TM, exhibiting ~70% recovery rate (Figure 1B). In parallel, we examined the recovery rate of seedlings upon pretreatment with another ER stress inducer, dithiothreitol (DTT, a reducing agent that blocks disulfide bridge formation). Consistently, *rtp1* mutants exhibited much less recovery rate in comparison to WT Col-0, while the recovered seedlings in *RTP1*-OE transgenic lines were increased to the comparable level of WT Col-0 (Figure 1C). These results imply that *RTP1* is involved in the TM- and DTT-induced ER stress responses.

To further examine whether *RTP1* regulates ER stress sensing and the subsequent UPR signaling, 2-week-old WT Col-0 and *rtp1* mutant seedlings were treated with TM and the transcript levels of ER stress sensor genes *bZIP28* and *bZIP60*, as well as UPR marker genes *BiP3* and *DnaJ* (ER stress-induced genes, participating in ER-localized protein folding; Iwata et al., 2008) were analyzed by reverse transcription quantitative PCR (RT-qPCR). The results showed that expressions of *bZIP60*, *BiP3*, and *DnaJ* were clearly induced in WT Col-0 upon treatment of TM. In comparison, levels of their expressions were significantly increased in TM-treated *rtp1* mutants, particularly at 12-h post treatment (Figure 1D). Although the expression of *bZIP28* was slightly induced by TM treatment, its transcript level was elevated in *rtp1* mutants compared with WT Col-0 (Figure 1D). Collectively, these results indicate that *RTP1* functions in general ER stress and UPR regulation.

RTP1 negatively modulates activation of UPR and ER stress-responsive plant immunity during infection by *P. parasitica*

To further investigate whether *RTP1* functions in UPR signaling in *A. thaliana* upon infection by *P. parasitica*, 2-week-old WT Col-0 and *rtp1* mutant seedlings were inoculated with *P. parasitica* zoospores and the transcript levels of ER stress sensor genes *bZIP28*, *bZIP60*, as well as UPR marker genes *BiP3* and *DnaJ* in WT Col-0 and *rtp1* mutants during early colonization of *P. parasitica* were analyzed by RT-qPCR. The results showed expression of *bZIP28*, *bZIP60*, *BiP3*, and *DnaJ*

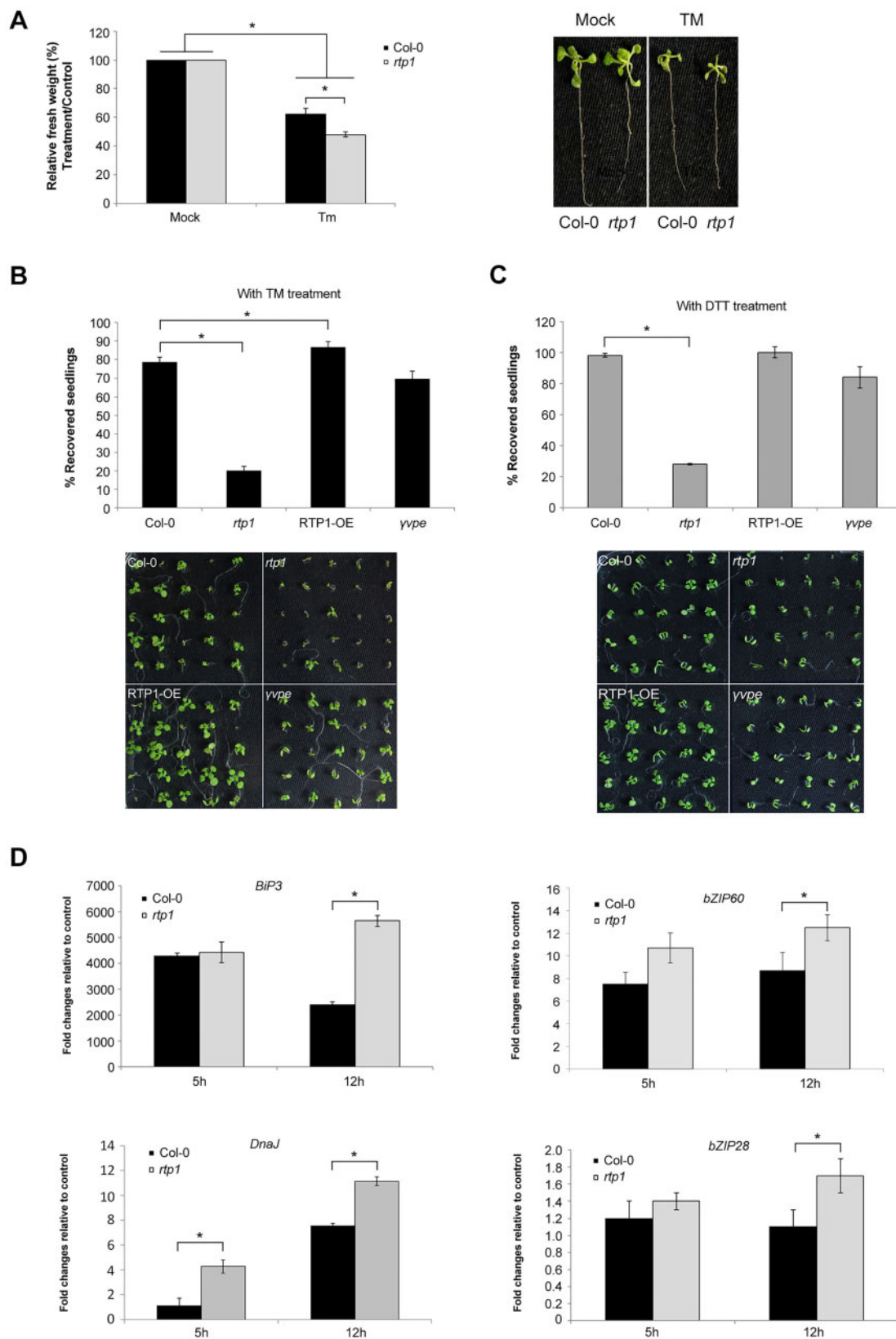


Figure 1 *RTP1* is involved in sensing TM- or DTT-induced ER stress and UPR regulation. A, The *A. thaliana* WT Col-0 and *rtp1* mutants show reduced biomass upon treatment by ER stress inducer TM. Plant biomass was determined at 5 d post treatment. Relative fresh weight was plotted by calculating the biomass of treatment/control seedlings. Data presented show means of three independent experiments \pm SE. For each experiment, 20 plants were analyzed per treatment. Asterisks indicate significance at $*P < 0.05$ analyzed by Student's *t* test. The phenotype of Col-0 and *rtp1* mutant seedlings at 5 d post treatment by TM was recorded. B and C, *Arabidopsis thaliana* seedlings of WT Col-0, *rtp1* mutants,

was induced in WT Col-0 during the early colonization (Figure 2A). In comparison, we found generally increased expression of these genes in *P. parasitica*-colonized *rtp1* mutants. For instance, expression levels of *BiP3* and *DnaJ* were significantly elevated in *rtp1* mutants at 3 and 12 hpi, respectively, compared with those in WT Col-0 (Figure 2A). To complement this, we further examined the level of BiP protein accumulation in both WT Col-0 and *rtp1* mutants colonized by *P. parasitica*. Similarly, the BiP protein accumulation was increased in *rtp1* mutants by 73% and 76% at 3 and 12 hpi, respectively, compared with that in WT Col-0 (Figure 2B). Furthermore, we found that the expression levels of both *bZIP28* and *bZIP60* were significantly increased in *rtp1* mutants at 24 hpi, compared with WT Col-0 (Figure 2A). These results indicate that plant UPR signaling is activated upon early infection by *P. parasitica*, while *RTP1* participates in modulating UPR activation in response to infection.

This prompted us to elucidate whether *RTP1* plays a regulatory role in synergistic signaling between UPR and plant immunity. As *rtp1* plants show broad spectrum resistance against biotrophic pathogens accompanied with faster accumulation of *PR1* transcripts, a key SA signaling marker gene (Pan et al., 2016), we further examined transcript levels of several immune-related genes in SA defense signaling and PTI pathways, including *WRKY33* (UPR-mediated SAR priming gene; Wakasa et al., 2014), *WRKY46* (SA signaling marker gene; Hu et al. 2012), *CBP60g* (SA signaling marker gene; Truman and Glazebrook, 2012), *MPK11* (SA signaling marker gene and PTI marker gene, encoding a MAP kinase activated during PTI; Bethke et al., 2012) and *CYP71A12* (PTI marker gene; Millet et al., 2010). The results showed that transcripts of all these immune genes were upregulated in WT Col-0 plants upon infection by *P. parasitica*. In comparison, stronger induction of expression of these genes was detected in *P. parasitica*-infected *rtp1* mutants, especially during the early biotrophic infection stage (Figure 2C).

Notably, based on our analyses on differentially expressed genes according to the RNA-seq data from WT Col-0 with treatment of TM and DMSO (control), the strongly induced immune genes (e.g. *WRKY33*, *WRKY46*, *CBP60g*, *MPK11*, and *CYP71A12*) in response to *P. parasitica* were identified to be simultaneously induced by TM (Supplemental Table S1). We assume that these genes are ER stress-responsive genes that may function in plant defense response against *P. parasitica*. Collectively, these data

imply that *RTP1* may play a negative regulating role in ER stress-mediated plant immunity, especially during the early biotrophic colonization stage.

RTP1 negatively regulates bZIP60 splicing activity and stabilizes ER membrane-associated bZIP60 TF

To further investigate how *RTP1* regulates plant UPR signaling pathways for functional integration with plant immunity, we firstly investigated whether *RTP1* might affect cytoplasmic splicing of the mRNA encoding the bZIP60 TF, which is a hallmark event in IRE1/bZIP60 mediated UPR signaling pathway. Two-week-old WT Col-0 and *rtp1* mutant seedlings were treated with TM and the bZIP60 splicing activity in TM-treated Col-0 and *rtp1* mutant plants were analyzed by quantitative transcript measurement that can distinguish between the forms of unspliced bZIP60 (*ubZIP60*) and spliced bZIP60 (*sbZIP60*, ER stress-activated form of bZIP60; Moreno et al., 2012). The results showed that bZIP60 splicing activity was significantly increased in TM-treated *rtp1* mutants, with ~20% and 40% more than that in WT Col-0 at 5-h and 12-h post treatment, respectively (Figure 3A), suggesting that *RTP1* plays a role in regulating bZIP60 processing upon TM-induced ER stress.

To further elucidate to what extent *RTP1* affects bZIP60 processing upon early infection by *P. parasitica*, we examined bZIP60 splicing activity in WT Col-0 and *rtp1* mutant plants colonized by *P. parasitica*, with seedlings of 2-week-old WT Col-0 and *rtp1* mutants inoculated with *P. parasitica* zoospores at 3, 6, 12, and 24 hpi. Similarly, the quantitative transcript measurement showed an increased bZIP60 splicing activity in *P. parasitica*-colonized *rtp1* mutants, with almost two-fold as that in WT Col-0 at 24 hpi (Figure 3B). These results imply that *RTP1* seems to negatively regulate bZIP60 processing upon infection by *P. parasitica*.

To examine whether the protein encoded by *RTP1* contributes to stabilization of the ER membrane-associated bZIP60 TF, the p35S::myc-bZIP60 construct or p35S::myc-GFP construct as a control was cotransformed with p35S::RTP1-FLAG or empty vector (EV) into *Nicotiana benthamiana* leaves by agroinfiltration. At 2- and 3-d post infiltration, the leaf protein was extracted and equal amount of proteins for each sample was used to evaluate the impact of *RTP1* on bZIP60 protein stability. The immunoblotting (IB) analysis showed that the accumulation of bZIP60 was significantly

Figure 1 (Continued)

RTP1-OE lines, and *γvpe* mutants were grown on 1/2 MS medium containing 0.3 μg/mL TM (B) and 2mM DTT (C) for 3 d. Percentage of recovery was plotted by calculating alive/dead seedlings recovered 10 d post TM treatment. Data presented show means of three independent experiments ± SE. For each experiment, 25 plants were analyzed per line. Asterisks indicate significance at **P* < 0.05 analyzed by Student's *t* test. D, Expressions of *BiP3*, *DnaJ*, *bZIP60*, and *bZIP28* were evaluated by RT-qPCR. Two-week-old *A. thaliana* WT Col-0 and *rtp1* mutant roots were treated with TM (5 μg/mL) or DMSO (control). Total RNA was extracted from treated root samples at 5 and 12 h post treatment. Data shown represent fold changes of genes and display the ratio of candidate gene expression to plant housekeeping gene *AtUBIQUITIN9* using the $\Delta\Delta$ Ct method in TM-treated plants relative to DMSO-treated plants. Three independent experiments showed similar results. Error bars indicate SE from three biological replicates. Asterisks indicate significance at **P* < 0.05 analyzed by Student's *t* test.

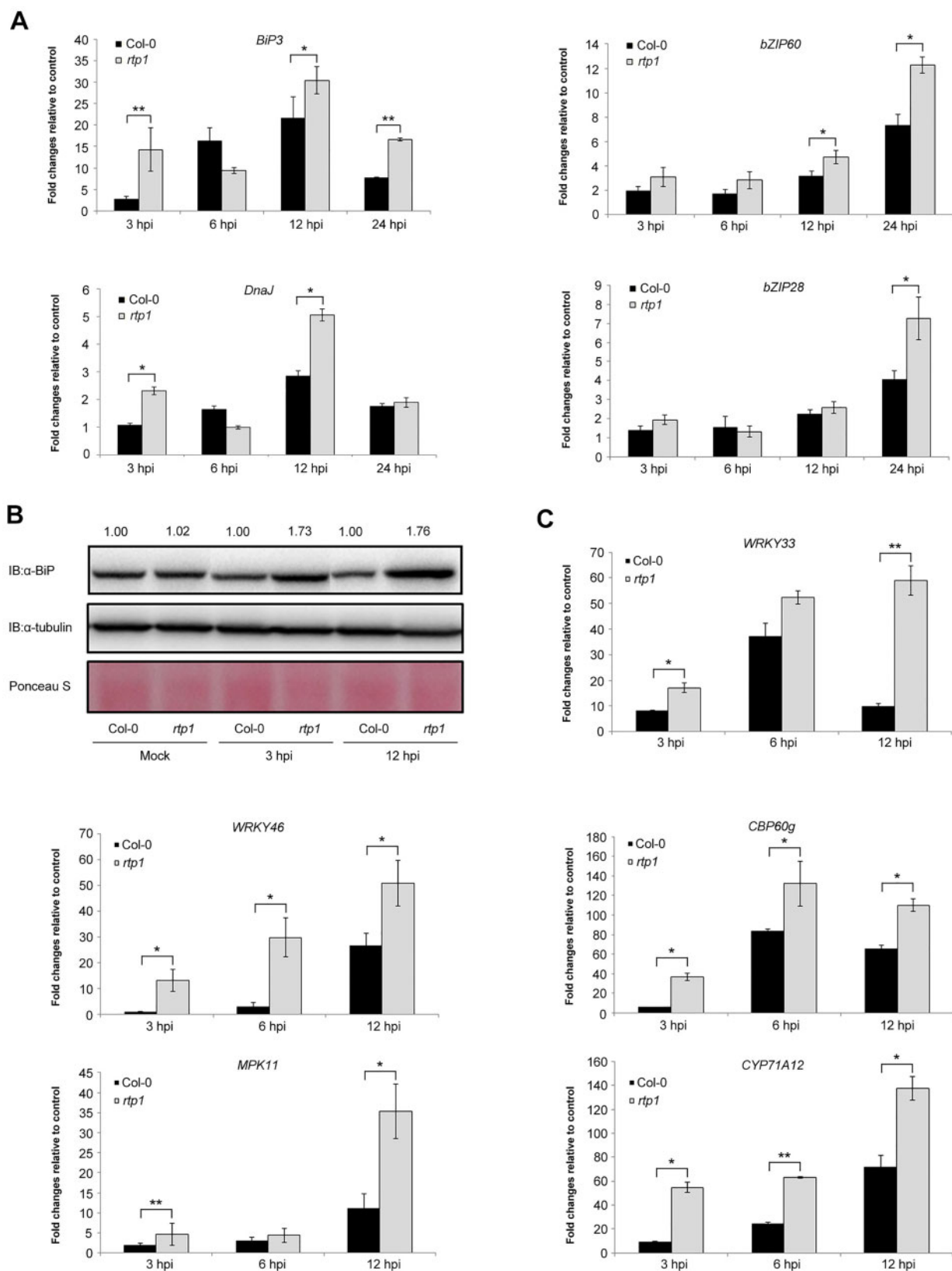


Figure 2 The *rtp1* mutants show stronger induction of UPR and ER stress-responsive immunity during the early infection by *P. parasitica*. **A**, Expressions of *BIP3*, *DnaJ*, *bZIP60*, and *bZIP28* were evaluated by RT-qPCR. Two-week-old *A. thaliana* WT Col-0 and *rtp1* mutant roots were dip-inoculated by *P. parasitica* zoospores or mock treated. Total RNA was extracted from inoculated roots at 3, 6, 12, and 24 hpi. Data shown represent fold changes of genes and display the ratio of candidate gene expression to plant housekeeping gene *AtUBIQUITIN9* using the $\Delta\Delta C_t$ method in colonized plants relative to mock-treated plants. Fold changes >1 indicate induction of genes. Data presented show means of three independent experiments

increased when coexpressed with RTP1 compared with that of EV control, with an increase of almost 2- and 2.81-fold protein accumulation at 2- and 3-d post coinfiltration, respectively (Figure 3, C and D), whereas the accumulation of GFP protein was not affected in the presence of RTP1 (Supplemental Figure S1). This suggests that RTP1 stabilizes

the ER membrane-associated bZIP60 TF. Consistent with this finding, when we coexpressed either mCherry-bZIP60 with RTP1-GFP or GFP-bZIP60 with mCherry-labeled ER marker in *N. benthamiana* leaves, the confocal microscopy showed overlapping of mCherry-bZIP60 with RTP1-GFP (Supplemental Figure S2, A and B) as well as GFP-bZIP60

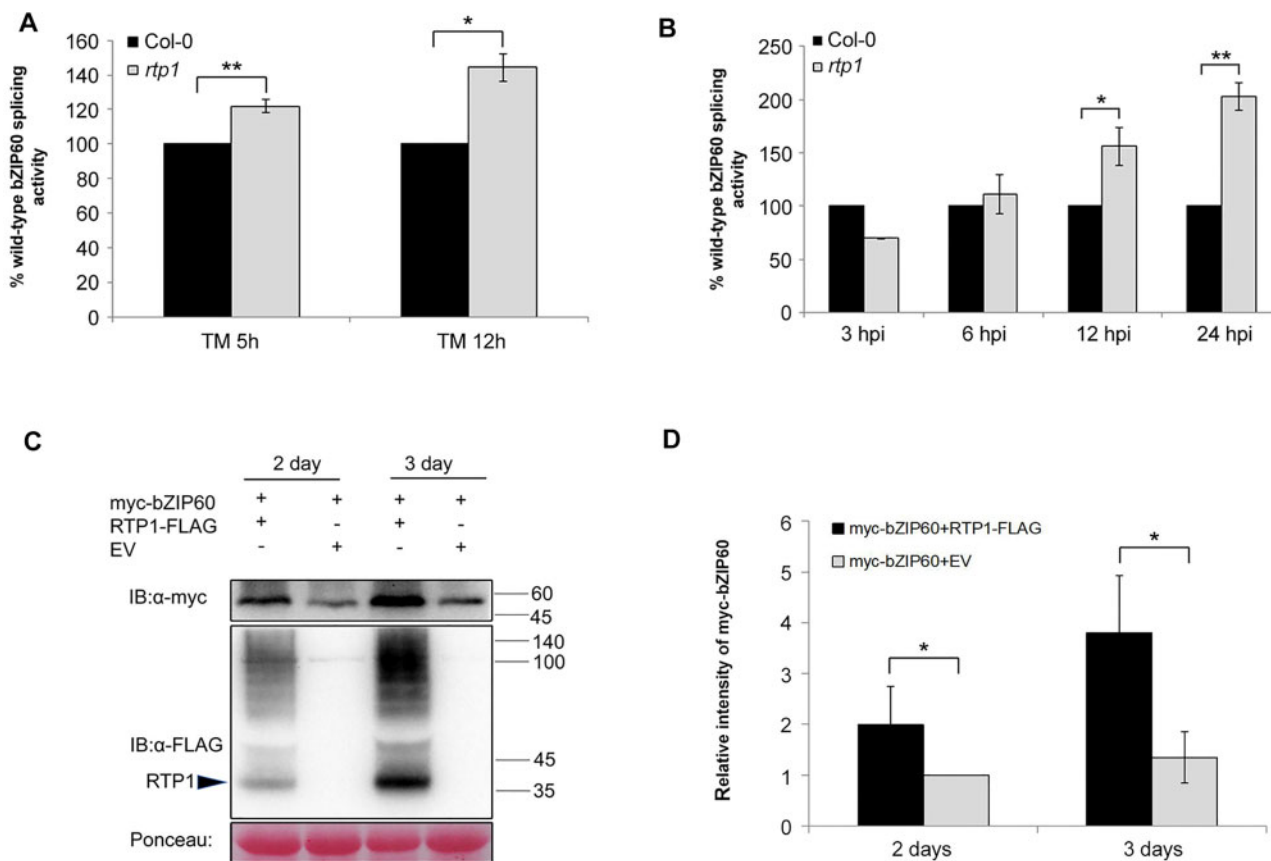


Figure 3 RTP1 negatively regulates bZIP60 splicing activity and stabilizes ER membrane-localized bZIP60 transcription factor. A and B, The bZIP60 splicing activity was evaluated by RT-qPCR. Ten-day-old *A. thaliana* Col-0 and *rtp1* mutant roots were treated by 5 μ g/mL TM (A) or dip-inoculated by *P. parasitica* zoospores (B) and harvested at indicated time points. Total RNA was extracted and *AtUBIQUITIN9* was used as the plant reference gene. Ratios of fold induction of spliced and unspliced *bZIP60* were plotted, while setting ratio of Col-0 as 100%. Data presented show means of three independent experiments \pm SE. Asterisks indicate significance at * P < 0.05 and ** P < 0.01 analyzed by Student's *t* test. C, Protein stability of bZIP60, coexpressed with RTP1 or empty vector, was analyzed by IB. Total proteins were extracted from infiltrated leaves at 2- and 3-d post infiltration. The accumulation of 7 \times myc-bZIP60 and RTP1-3 \times FLAG was detected by IB using anti-myc- and anti-FLAG- antibodies, respectively. The protein size of RTP1 was marked by arrowhead. D, Relative myc-bZIP60 protein band intensities (protein accumulation at 2-d post infiltration, when coexpressed 7 \times myc-bZIP60 and EV, was set to 1) were determined by Image J. Ponceau staining of the membrane was used to show equal loading. Data presented show means of three independent experiments \pm SE. Asterisks indicate significance at * P < 0.05 analyzed by Student's *t* test.

Figure 2 (Continued)

\pm SE. Asterisks indicate significance at * P < 0.05 and ** P < 0.01 analyzed by Student's *t* test. B, BiP protein accumulation is increased in *rtp1* mutant during early infection by *P. parasitica*. Two-week-old *A. thaliana* Col-0 and *rtp1* mutant roots were dip-inoculated by *P. parasitica* zoospores or mock treated and harvest at 3 and 12 hpi for protein extraction. The antibody against α -tubulin was used to probe the total protein in blot to confirm equal loading of the samples. Numbers on top of the immunoblot indicate relative BiP protein band intensities (Col-0 Mock was set to 1) as determined by Image J. The experiment was repeated three times with similar results. C, Expressions of ER stress-responsive immune genes *WRKY33*, *WRKY46*, *CBP60g*, *MPK11*, and *CYP71A12* were evaluated by RT-qPCR. Two-week-old *A. thaliana* WT Col-0 and *rtp1* mutant roots were dip-inoculated by *P. parasitica* zoospores or mock treated. Total RNA was extracted from inoculated roots at 3, 6, and 12 hpi. Data shown represent fold changes of genes and display the ratio of candidate gene expression to plant housekeeping gene *AtUBIQUITIN9* using the $\Delta\Delta$ Ct method in colonized plants relative to mock-treated plants. Fold changes >1 indicate induction of genes. Three independent experiments showed similar results. Error bars indicate SE from three biological replicates. Asterisks indicate significance analyzed by Student's *t* test (* P < 0.05, ** P < 0.01).

with mCherry-labeled ER marker (Supplemental Figure S2, C and D), indicating the colocalization of bZIP60 and RTP1 in the ER.

RTP1 modulates the induction of *A. thaliana* IRE1 upon *P. parasitica* infection and manipulates the phosphorylation of IRE1 protein

The activation of bZIP60 requires unconventional splicing of bZIP60 mRNA executed by ER membrane-associated protein IRE1. IRE1 contains a PK domain and a ribonuclease domain, which is an important UPR regulator in plants (Nagashima et al., 2011). Therefore, we further examined whether *RTP1* is involved in regulating the induction pattern of *IRE1* under TM-induced ER stress and upon *P. parasitica* infection. The RT-qPCR results showed that the expression of *IRE1a* was not obviously induced in either WT Col-0 or *rtp1* mutants upon treatment by TM at 5 h and 12 h. In comparison, the expression of *IRE1b* was significantly induced in TM-treated *rtp1* mutants at 12 h (Figure 4, A and B). Interestingly, the transcript levels of both *IRE1a* and *IRE1b* exhibited slight elevation in *P. parasitica*-colonized WT Col-0 at 3 hpi, followed by a gradual reduction during the infection. Nevertheless, the induction peaks of *IRE1a* and *IRE1b* did not occur until 12 hpi in *P. parasitica*-colonized *rtp1* mutants. Meanwhile, higher levels of *IRE1a* and *IRE1b* transcripts were notable in *rtp1* mutants at 12 and 24 hpi, respectively, compared with those in WT Col-0 (Figure 4, C and D). In accordance with this, quantification of *P. parasitica* biomass by qPCR showed significantly much less pathogen colonization at 12 and 24 hpi in *rtp1* mutants compared with Col-0 (Figure 4E). These results imply that *RTP1* is involved in modulating the expression pattern of *IRE1* in *A. thaliana* during the early stage of colonization by *P. parasitica*.

The isoforms of IRE1a and IRE1b in *A. thaliana* are classified as a single-pass transmembrane protein in the ER membrane and their activation seems to be induced by its trans-autophosphorylation (Koizumi et al., 2001; Zhang et al., 2016). To elucidate whether the ER membrane-localized protein encoded by *RTP1* could affect the phosphorylation activity of IRE1, we cotransformed the constructs of p35S::*IRE1a*-FLAG with p35S::*RTP1*-HA or p35S::*EV* as well as p35S::*FLAG*-*IRE1b* with p35S::*RTP1*-HA or p35S::*EV*, using *Agrobacterium*-mediated transient transformation in leaves of *N. benthamiana*. At 3-d post coinfiltration, phosphorylated and unphosphorylated forms of IRE1 were analyzed as described (Kinoshita et al., 2006). The IB results showed that when coexpressed with EV, both IRE1a and IRE1b exhibited clear phosphorylated forms of the protein, with a size of ~130 kDa, indicative of the IRE1 phosphorylation (Figure 4F; Supplemental Figure S3). Interestingly, analysis of relative intensities of phosphorylated IRE1 proteins showed that the phosphorylated form of IRE1b was obviously reduced when coexpressed with *RTP1*, being around 50% less than that coexpressed with EV, though the

phosphorylated form of IRE1a appeared less affected by *RTP1* (Figure 4F; Supplemental Figure S3).

As both phosphorylated and unphosphorylated forms of IRE1 were attenuated when coexpressed with *RTP1* (Figure 4F; Supplemental Figure S3), we further examined whether *RTP1* affects the stability of IRE1 proteins through *Agrobacteria*-mediated transient cotransformation in *N. benthamiana* leaves. The IB results exhibited that the accumulation of both IRE1a and IRE1b was significantly reduced when coexpressed with *RTP1* compared with that coexpressed with EV at 3-d post coinfiltration (Supplemental Figure S4). Taken together, these in vivo assays imply that *RTP1* is involved in manipulating the general phosphorylation of IRE1b and stability of IRE1 proteins, though the interactions between *RTP1* and IRE1a or IRE1b were not detected (Figure S5).

RTP1 interacts with and stabilizes ER membrane-associated bZIP28

To further investigate how *RTP1* manipulates the induction of plant UPR pathway mediated by the ER-membrane localized stress sensor bZIP28, we analyzed whether *RTP1* interacts with bZIP28 protein using the firefly luciferase complementation imaging assay. The constructs of *RTP1*-NLuc and CLuc-bZIP28, *RTP1*-NLuc and CLuc, NLuc and CLuc-bZIP28, NLuc and CLuc were cotransformed in leaves of *N. benthamiana*, respectively, and the relative luciferase activities were measured and recorded at 3-d post cotransformation (Chen et al., 2008). Our results showed that coexpression of *RTP1*-NLuc and CLuc, NLuc and CLuc-bZIP28, NLuc and CLuc did not show luciferase complementation signals, whereas coexpression of *RTP1*-NLuc and CLuc-bZIP28 resulted in strong luciferase complementation signal (Figure 5A), implying that the protein encoded by the full-length bZIP28 interacts with *RTP1*.

To further confirm this interaction, we carried out co-immunoprecipitation (Co-IP) assays. The p35S::*myc*-bZIP28 construct was cotransformed with either p35S::*RTP1*-FLAG or p35S::*FLAG*-GFP in *N. benthamiana* leaves through agroinfiltration. Total proteins were extracted from infiltrated leaves and were immunoprecipitated with FLAG-Trap agarose beads. The IB results showed that myc-bZIP28 was co-immunoprecipitated in *RTP1*-FLAG-expressed samples, but not in the FLAG-GFP samples, though it was expressed in all leaves (Figure 5B). These results were further confirmed by the Co-IP of *RTP1*-FLAG in myc-bZIP28-expressed samples, but not in the myc-GFP samples, using anti-myc magnetic beads, when we cotransformed p35S::*RTP1*-FLAG construct with either p35S::*myc*-bZIP28 or p35S::*myc*-GFP in *N. benthamiana* leaves (Supplemental Figure S6). Taken together, these results indicate that *RTP1* interacts with ER stress-sensing TF bZIP28 in planta.

To further elucidate whether *RTP1* targeting stabilizes bZIP28, the myc-bZIP28 fusion construct was cotransformed with *RTP1*-FLAG or EV into *N. benthamiana* leaves by

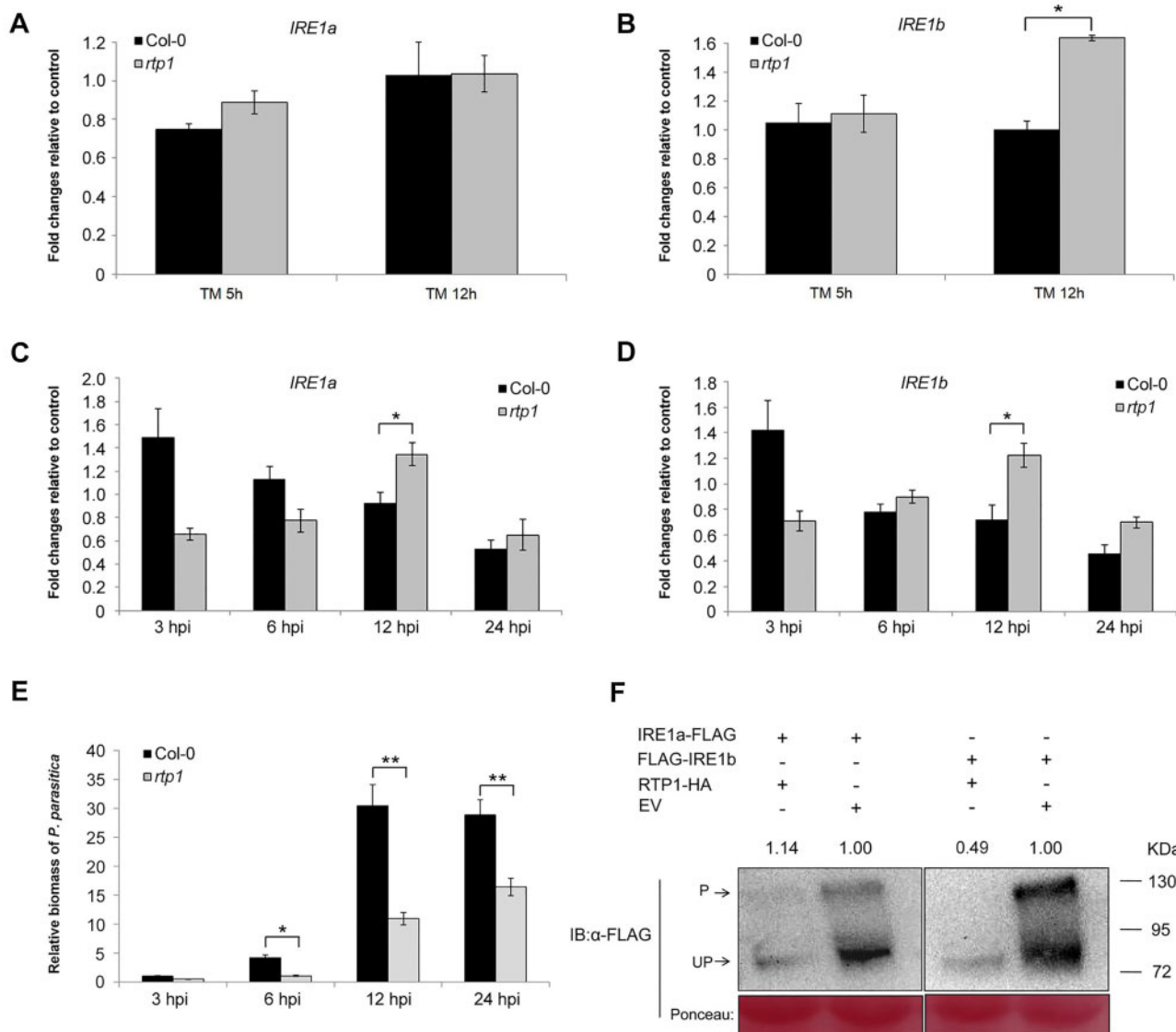


Figure 4 RTP1 modulates the induction of *A. thaliana* IRE1 upon *P. parasitica* infection and manipulates the phosphorylation of IRE1. A–D, Expressions of *IRE1a* and *IRE1b* was evaluated by RT-qPCR. Ten-day-old *A. thaliana* Col-0 and *rtp1* mutant roots were treated by 5 μ g/mL TM (A and B) or dip-inoculated by *P. parasitica* zoospores (C and D). Total RNA was extracted from treated or inoculated roots at indicated time points. Data shown represent fold changes of genes and display the ratio of candidate gene expression to plant housekeeping gene *AtUBIQUITIN9* using the $\Delta\Delta C_t$ method in TM-treated or colonized plants relative to DMSO- or mock-treated plants. Data presented show means of three independent experiments \pm SE. Asterisks indicate significance at * $P < 0.05$ analyzed by Student's *t* test. E, Quantification of *P. parasitica* biomass in *A. thaliana* Co-0 and *rtp1* mutant roots at 3, 6, 12, and 24 hpi was determined by RT-qPCR. Primers specific for the *P. parasitica* UBC and the *AtUBIQUITIN9* were used. For each experiment, approximately 200 plants were analyzed per line. Bars represent *PpUBC* levels relative to *AtUBC9* levels with SE of three biological replicates. Asterisks denote significance in the colonization of *rtp1* mutant compared with Col-0 analyzed by Student's *t* test (* $P < 0.05$; ** $P < 0.01$). F, The phosphorylation levels of IRE1a-3 \times FLAG and 3 \times FLAG-IRE1b, coexpressed with RTP1-HA or empty vector, was analyzed by IB. Total proteins were extracted from infiltrated leaves at 3-d post agroinfiltration and then separated by phosphate affinity SDS-PAGE in a 7.5% (w/v) polyacrylamide gel containing 15M Phos-tag. The phosphorylated or unphosphorylated IRE1a-3 \times FLAG and 3 \times FLAG-IRE1b were detected by IB using anti-flag antibody. Two independent experiments were performed showing similar results. The band intensities of P and UP were determined by the gray values using Image J. The adjusted band intensities of P in the tested samples (i.e. IRE1a-FLAG or FLAG-IRE1b + RTP1-HA) were calculated as described in M&M. Protein loading is indicated by Ponceau staining. Numbers on top of the immunoblot indicate adjusted band intensities of P in the tested samples normalized to band intensities of P in the control samples (i.e. IRE1a-FLAG or FLAG-IRE1b + EV). UP, unphosphorylated IRE1; P, phosphorylated IRE1.

agroinfiltration. At 2- and 3-d post infiltration, the leaf proteins were extracted and equal amount of proteins for each sample was used to evaluate the impact of RTP1 on bZIP28 protein stability. The IB analysis showed that the

accumulation of bZIP28 was significantly increased when coexpressed with RTP1 compared to that coexpressed with EV, with an increase of 73% and two-fold protein accumulation at 2- and 3-d post coinfiltration, respectively (Figure 5,

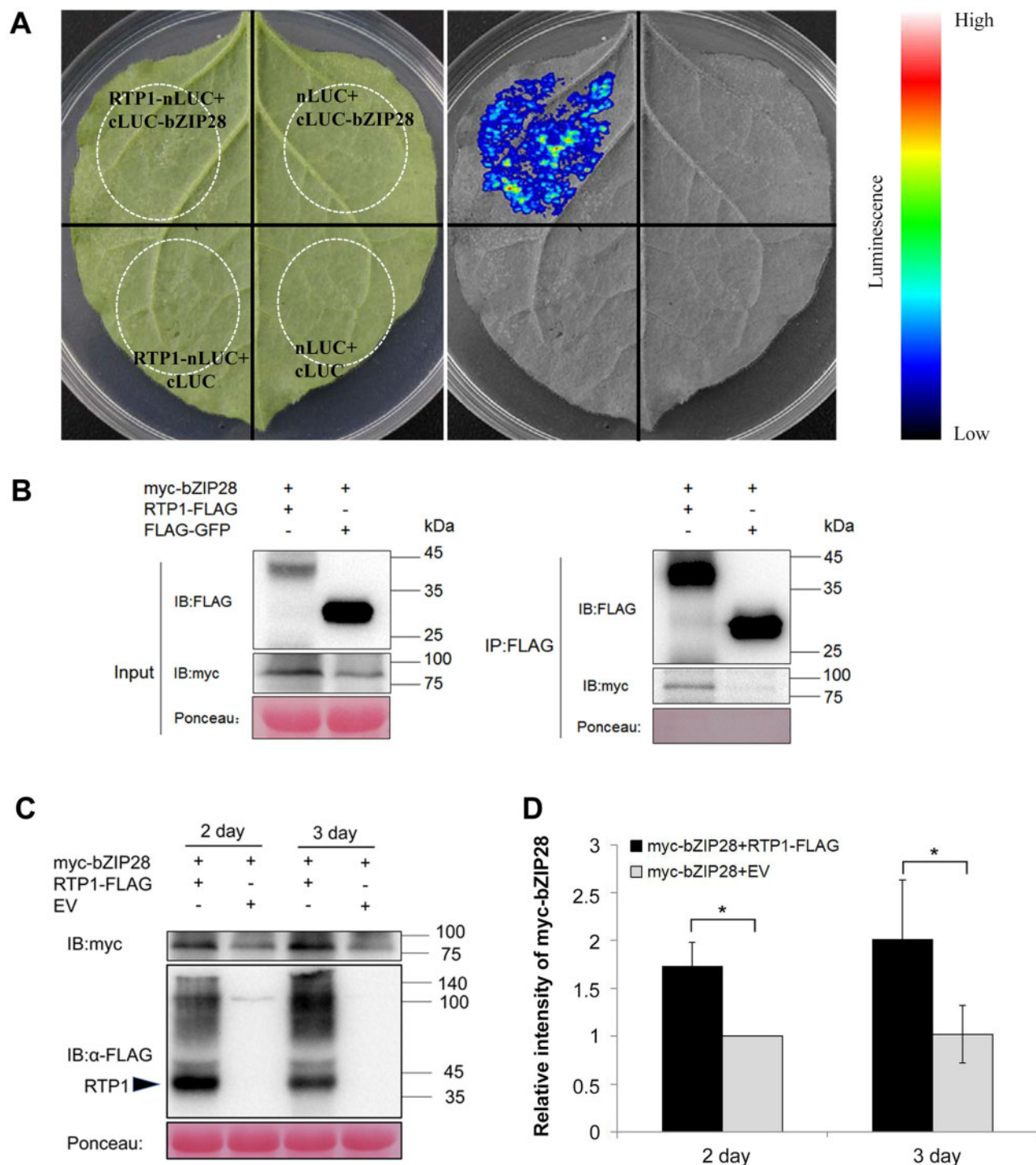


Figure 5 RTP1 interacts with and stabilizes bZIP28. Proteins were expressed in *N. benthamiana* leaves through infiltration with an *A. tumefaciens* cell suspension with an OD₆₀₀ value of 0.3. A, The interaction between RTP1 and bZIP28 in living cells was detected by firefly luciferase complementation imaging assay at 72-h post infiltration. The N terminus of LUC was fused to the C terminal of RTP1, and the C terminus of LUC was fused to the N terminus of bZIP28. Coexpression of RTP1-nLUC and cLUC-bZIP28 resulted in specific fluorescence as detected by a low-light cooled charge-coupled device camera. Three independent biological experiments were performed and showed similar results. B, CoIP assays showing that RTP1 interacts with bZIP28 *in planta*. Total native protein extracts (input) from agroinfiltrated leaves expressing the indicated proteins were precipitated with anti-FLAG M2 affinity gel (IP: FLAG), separated on SDS-PAGE gels, and blotted with specific antibodies. In immunoprecipitation fractions, 7×myc-bZIP28 was detected in a complex with RTP1-3×FLAG, but not with FLAG-GFP. Protein size markers are indicated in kDa, and protein loading is indicated by Ponceau staining. Three independent biological experiments were performed and showed similar results. C, Protein stability of bZIP28, coexpressed with RTP1 or empty vector, was analyzed by IB. Total proteins were extracted from infiltrated leaves at 2- and 3-d post infiltration. The accumulation of 7×myc-bZIP28 and RTP1-3×FLAG was detected by IB using anti-myc- and anti-FLAG antibodies, respectively. The protein size of RTP1 was marked by arrowhead. D, Relative bZIP28 protein band intensities (protein accumulation at 2-d post

C and D), indicating that targeting of ER membrane-associated bZIP28 by RTP1 enhances its stability.

Both bZIP60 and bZIP28 are required for *rtp1*-mediated plant resistance against *P. parasitica*

To investigate the potential function of the key UPR regulators bZIP60 and bZIP28 in *rtp1*-mediated plant resistance, we generated *rtp1bzip60* and *rtp1bzip28* double mutants by crossing *rtp1* with *bzip60* as well as *bzip28* mutants. The detached leaves of 6-week-old mutants of *bzip60*, *bzip28*, *rtp1bzip60*, and *rtp1bzip28* were compared with WT Col-0 and *rtp1* mutant following inoculation with *P. parasitica* zoospores. At 48 hpi, leaves of both *bzip60* and *bzip28* mutants displayed severer water-soaked lesions compared with that exhibited in WT Col-0, whereas *rtp1* mutant showed less visible lesions (Figure 6A). Both disease index statistics and qPCR assay for pathogen biomass (Figure 6, B and C) consistently indicated that both *bzip60* and *bzip28* mutants were more susceptible than WT Col-0 to *P. parasitica* infection, suggesting their potential functions in plant resistance. In parallel, both *rtp1bzip60* and *rtp1bzip28* double mutants were significantly more susceptible to *P. parasitica* than the *rtp1* mutant, though they exhibited less susceptibility than either *bzip60* or *bzip28* mutant (Figure 6, A and B). Quantification of *P. parasitica* biomass confirmed that the resistance of *rtp1* mutant clearly compromised in both *rtp1bzip60* and *rtp1bzip28* double mutants, in which the level of *P. parasitica* colonization was dramatically higher than in *rtp1* mutant but less than in mutants of *bzip60* and *bzip28* (Figure 6C). These results indicate that UPR regulators bZIP60 and bZIP28 play a role in *rtp1*-mediated plant resistance against *P. parasitica* and they may function downstream of RTP1.

Both bZIP60 and bZIP28 play a role in the activation of ER stress-responsive immunity in *rtp1* plants

The expression of several ER stress-responsive immune genes (e.g. *WRKY33*, *WRKY46*, *CBP60g*, *MPK11*, and *CYP71A12*; Supplemental Table S1) showed stronger induction in *rtp1* mutants than in WT Col-0 upon early infection by *P. parasitica* (Figure 2C), implying their potential shared function as novel UPR regulators and key components in RTP1-mediated immune signaling. Moreover, the significant induction of expression of these ER stress-responsive immune genes occurred simultaneously with increased expression of bZIP28 and bZIP60 in *P. parasitica*-infected *rtp1* mutants (Figure 2A). This prompted us to examine the activation of ER stress-responsive immunity in *rtp1* plants by bZIP60 and bZIP28. We performed RT-qPCR assay to examine transcript levels of these ER stress-responsive immune genes in WT Col-0, *rtp1*, *rtp1bzip60*, and *rtp1bzip28* upon early infection

by *P. parasitica*. In comparison to the stronger induction of expression of ER stress-responsive immune genes *WRKY33*, *WRKY46*, *CBP60g*, *MPK11*, and *CYP71A12* in *P. parasitica*-colonized *rtp1* mutant, transcript levels of these genes were notably reduced in double mutants *rtp1bzip60* and *rtp1bzip28* during the early stage of colonization by *P. parasitica* (Figure 7A), suggesting the regulatory roles of bZIP60 and bZIP28 in the activation of ER stress-responsive immune genes in *rtp1* during the infection.

As callose deposition and reactive oxygen species (ROS) production are characteristic of PTI mediated by the leucine-rich repeat receptor kinases flagellin-sensing 2 (FLS2; Luna et al., 2011), we assessed callose deposition and oxidative burst in leaves of WT Col-0 and *rtp1* mutants triggered by flg22, the cognate ligand of the FLS2 receptor. Using aniline-blue staining and fluorescence microscopy, more callose deposition was found in the leaves of *rtp1* mutant than that in WT Col-0 plants by 24 h of treatment (Figure 7, C and E). Simultaneously, luminol-based assay confirmed a stronger transient oxidative burst in *rtp1* mutants than in WT Col-0 (Figure 7B). Further analyses on mutants of *bzip60*, *bzip28*, *rtp1bzip60*, and *rtp1bzip28* upon flg22 treatment showed that oxidative burst was obviously abolished in *bzip60* and *bzip28* mutants compared with that in WT Col-0. Moreover, the strong oxidative burst occurred in *rtp1* mutant was attenuated in *rtp1bzip60* and *rtp1bzip28* mutants (Figure 7B). These results suggest that RTP1 is involved in PAMP-triggered immune signaling, in which bZIP60 and bZIP28 might play a regulatory role. Consistently, visible callose deposition was monitored in WT Col-0 leaves upon early infection by *P. parasitica*, while *rtp1* mutants showed ~60% more callose deposition. Notably, both mutants *rtp1bzip28* and *rtp1bzip60* exhibited significantly less callose deposition than *rtp1* mutant (Figure 7, D and F), indicating its compromised defense response to pathogen infection. Collectively, these results point to the notion that both bZIP60 and bZIP28 play a role in *rtp1*-mediated plant resistance through their probable shared function to facilitate synergistic signaling of UPR and ER stress-mediated plant immunity.

Discussion

Host cells use an intricate signaling system to respond to invasions by pathogenic microorganisms. Although several signaling components of disease resistance against biotrophic pathogens have been identified, our understanding of molecular components and host processes that contribute to plant disease susceptibility remains elusive. The susceptibility factor RTP1 encodes an ER membrane-localized protein and negatively regulates plant resistance to biotrophic pathogens including *P. parasitica* (Pan et al., 2016). In this study, we further demonstrate a role of *A. thaliana* RTP1 in the UPR. Specifically, we establish the role of RTP1 in

infiltration, when coexpressed 7×myc-bZIP28 and EV, was set to 1) were determined by Image J. Ponceau staining of the membrane was used to show equal loading. Data presented show means of three independent experiments ± SE. Asterisks indicate significance at **P*<0.05 analyzed by Student's *t* test.

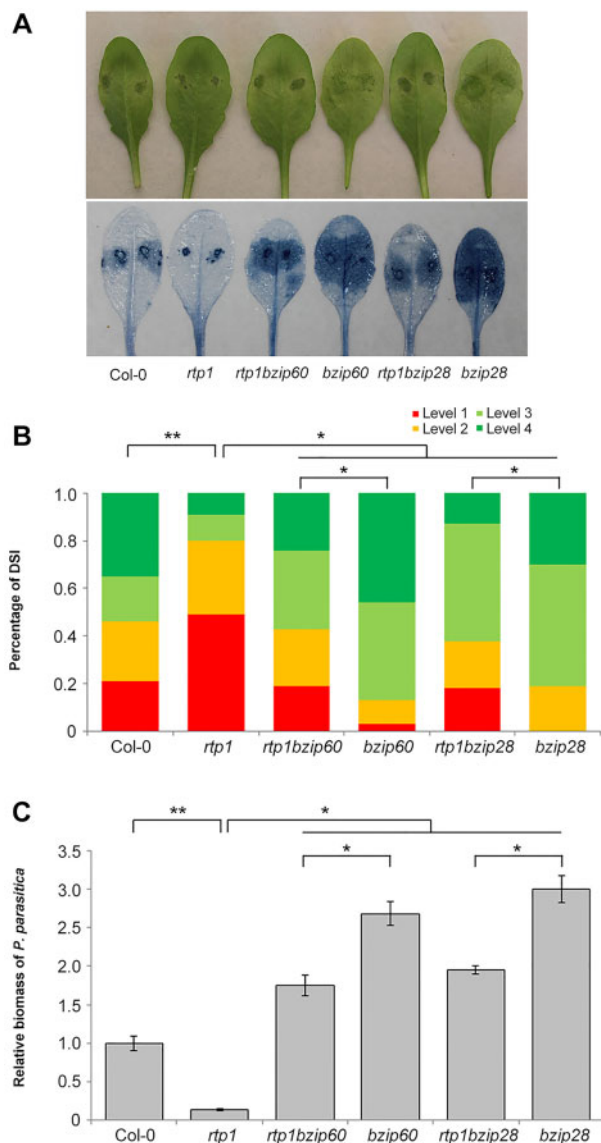
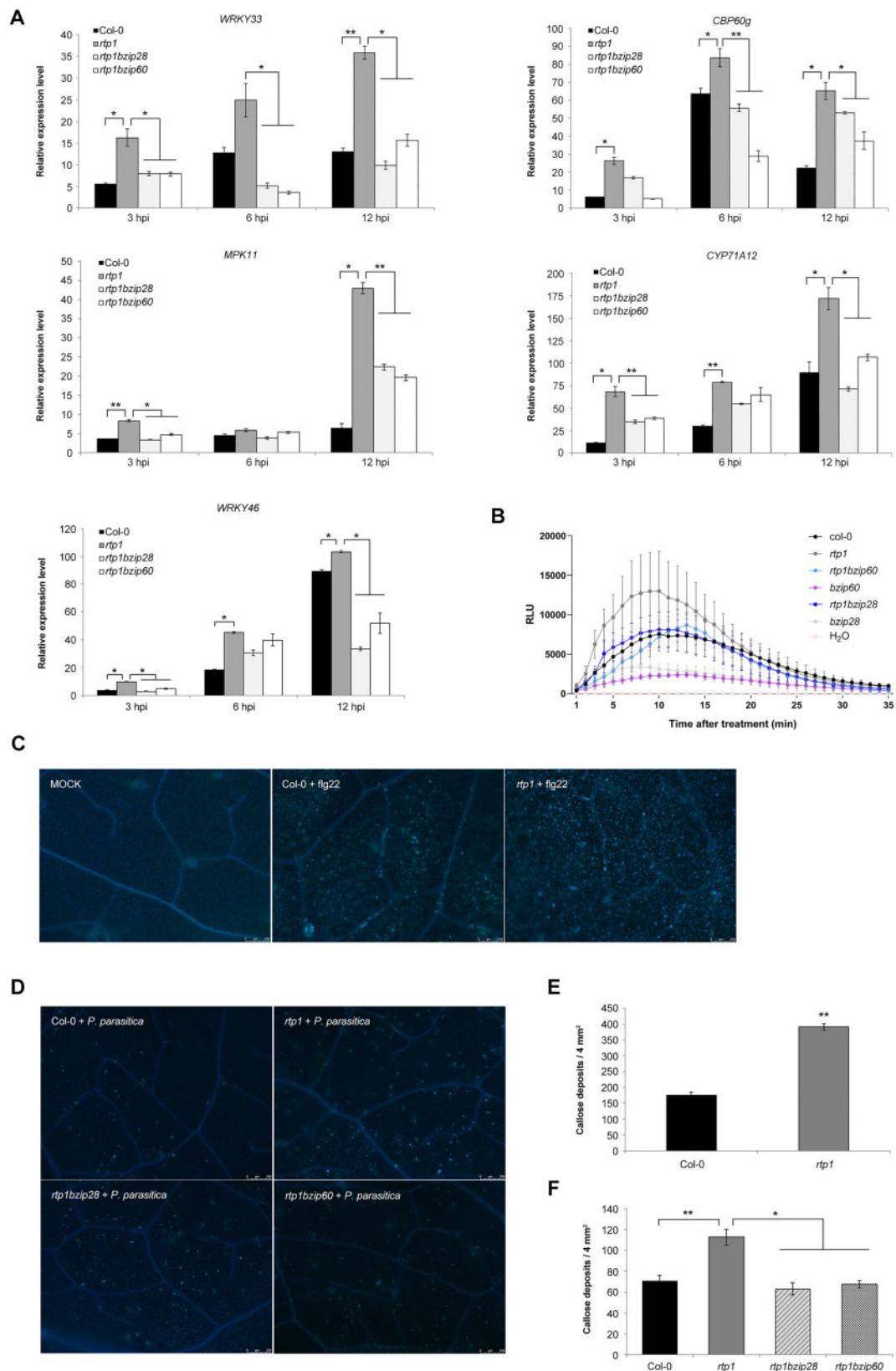


Figure 6 Both *bZIP60* and *bZIP28* are required for *rtp1*-mediated plant resistance against *P. parasitica*. **A**, Detached leaves of *bzip28* and *bzip60* mutants showed enhanced susceptibility and *rtp1* mutant exhibited resistance against infection by *P. parasitica*, compared to WT Col-0 plants. Detached leaves of *rtp1bzip60* and *rtp1bzip28* double mutants showed compromised resistance compared to *rtp1* mutant against *P. parasitica*. Representative images were taken at 48 hpi. **B**, Disease severity index (DSI) from level 1 to level 4 was recorded at 48 hpi. Level 1: disease symptom is less than 1/3 of whole leaf area; level 2: disease symptom is between 1/3 and 1/2 of whole leaf area; level 3: disease symptom is between 1/2 and 2/3 of whole leaf area; and level 4: disease symptom is more than 2/3 of whole leaf area. Asterisks indicate significant differences between genotypes (Wilcoxon rank-sum test: * $P < 0.05$, ** $P < 0.01$). **C**, Quantification of *P. parasitica* biomass in infected *A. thaliana* leaves at 48 hpi was determined by RT-qPCR. Primers specific for the *P. parasitica* UBC and the *AtUBIQUITIN9* were used. The biomasses of *P. parasitica* in all mutants were normalized with that in WT Col-0 (set to 1). For each experiment, approximately 200 plants were analyzed per line. Bars represent *PpUBC* levels relative to *AtUBC* levels with *se* of three biological replicates. Asterisks denote significance analyzed by student's *t* test (* $P < 0.05$; ** $P < 0.01$).

responding to TM- and DTT-induced ER stress, as demonstrated by altered tolerance to ER stress (Figure 1, A–C) and enhanced induction of UPR marker genes in *rtp1* mutants (Figure 1D). Consistently with these observations, induction of expression of UPR marker genes in *P. parasitica*-colonized Col-0 plants (Figure 2A) indicates UPR activation upon infection. In comparison, the increased expression of these UPR genes in *rtp1* mutant during infection (Figure 2A) suggests the role of *RTP1* as a negative regulator for UPR activation in *A. thaliana* upon colonization of *P. parasitica*.

There is increasing evidence that UPR signaling contributes to plant immunity in different ways, for instance, through the regulation of antimicrobial protein secretion, the processing of pattern-recognition receptors for PTI, the priming of SAR and ER stress-mediated cell death (Wang et al., 2005; Li et al., 2009; Moreno et al., 2012; Qiang et al., 2012). In addition to the stronger induction of UPR in *P. parasitica*-infected *rtp1* mutants (Figure 2, A and B), our study further suggests that *RTP1* participates in negative modulation of SA-mediated defense signaling, as demonstrated by the higher expression levels of SA-mediated immune genes in *rtp1* mutants than in WT Col-0 plants during the infection (Figure 2C). These results support the notion that *RTP1* negatively regulates plant resistance to biotrophic but not necrotrophic pathogens (Pan et al., 2016), as SA signaling is thought to be essential to resist infection from biotrophic pathogens (Dodds and Rathjen, 2010). Furthermore, plant hormone signaling pathways including SA signaling contribute positively to PTI and PTI strongly depends on synergistic interactions between these signaling pathways (Tsuda et al., 2009). Indeed, our results showed that induction of PAMP-activated genes (*CYP71A12* and *MPK11*; Millet et al., 2010; Bethke et al., 2012) as well as PAMP-elicited callose deposition and oxidative burst were dramatically increased in *rtp1* mutant plants compared to Col-0 upon early stage of infection (Figures 2, C and 7, B, C, and E), suggesting the potential function of *RTP1* in PTI. These data further support the finding that *RTP1*-mediated plant resistance is broad spectrum (Pan et al., 2016), as PTI is conserved in different plant species and acts as a basal defense (Lacombe et al., 2010). Moreover, the expression levels of the ER stress-mediated plant immune gene *EFR*, ER stress-mediated cell death gene γ VPE, and secreted immunity-related protein gene *PR1* were increased in *rtp1* mutant during the early stage of infection compared with that in Col-0 (Supplemental Figure S7; Pan et al., 2016). Collectively, these results indicate that *RTP1* negatively regulates plant resistance, most likely by participating in UPR signaling pathways.

As a master regulator of SA-mediated immune defense, NPR1 functions to antagonize the UPR regulators *bZIP28* and *bZIP60*, independent of its role in SA defense (Lai et al., 2018). This suggests the possibility of cross-signaling between UPR and SA-mediated defense through the critical modulator NPR1. Intriguingly, our study further reveals a scenario



that the immune function of RTP1 is highly associated with its role in modulating the ER membrane-bound UPR regulators bZIP28 and bZIP60. Through interacting with and stabilizing the ER membrane-tethered bZIP28 (Figure 5; Supplemental Figure S6), RTP1 possibly contributes to retain the bZIP28 in the ER. Additional subcellular localization assays also support their partial colocalization in the ER membrane (Supplemental Figure S8). We speculate that the activation of bZIP28 TF is probably manipulated by RTP1, as evident by the elevated induction of UPR in *rtp1* mutant in response to either TM treatment (Figure 1D) or pathogen infection (Figure 2, A and B).

In *A. thaliana*, bZIP60 is thought to transmit the ER stress signal in the UPR pathway through ER-localized IRE1, an RNA splicing enzyme (Iwata and Koizumi, 2012). AS *RTP1* loss-of-function enhances bZIP60 splicing activity induced either by TM treatment (Figure 3A) or upon infection by *P. parasitica* (Figure 3B), we speculate that RTP1 might be involved in manipulating bZIP60 mRNA processing. Further finding that the expression pattern of *IRE1* is associated with significantly enhanced bZIP60 splicing activity and reduced colonization of *P. parasitica* in *rtp1* mutants during the infection (Figures 3, B and 4, C–E) implies bZIP60 as a target of IRE1 nuclease activity in response to *P. parasitica* infection. Plant IRE1 is assumed to be activated by trans-autophosphorylation due to the presence of conserved cytosolic kinase and RNase domains among the eukaryotes (Koizumi et al., 2001; Zhang et al., 2016). Our findings that the general phosphorylation and stability of IRE1 protein are manipulated by RTP1 (Figure 4F; Supplemental Figures S3 and S4) provide evidence that RTP1 might negatively modulate the activation of RNA splicing enzyme IRE1. We speculate that the impact of RTP1 on differential phosphorylation between IRE1a and IRE1b (Figure 4F; Supplemental Figure S3) might be a consequence of their dissimilar PK activation loops (Koizumi et al., 2001). Further in vitro studies are of importance to understand the effect of RTP1 on the autophosphorylation of IRE1. Notably, though the direct interaction between RTP1 and IRE1 is not detected (Supplemental Figure S5), we find that RTP1 interacts with *A. thaliana* Bax inhibitor-1 (BI-1; Supplemental Figure S9). In mammalian cells, IRE1 α is demonstrated to interact with BI-1 to regulate its endoribonuclease activity (Lisbona et al., 2009). It remains to be examined whether BI-1 mediates interaction between RTP1 and IRE1. Consequently, it is logical to find that the ER membrane-associated bZIP60 is stabilized by RTP1 protein (Figure 3, C and D). Further finding that induction of

UPR is potentiated in *rtp1* mutant in response to either TM treatment (Figure 1D) or pathogen infection (Figure 2, A and B) suggests the activation of bZIP60 TF is manipulated by RTP1.

Increasing evidence indicate that IRE1/bZIP60-mediated UPR pathway not only functions in response to ER stress or heat stress (Iwata et al., 2008; Deng et al., 2011), but also may exert a unique role in certain biological processes such as plant–virus interactions and SA-mediated plant defense signaling in response to bacterial pathogens (Tateda et al., 2008; Moreno et al., 2012; Zhang et al., 2015). Our findings that *bZIP60* loss-of-function leads to increased susceptibility to *P. parasitica* indicate that the ER membrane-associated bZIP60 plays a role in the defense response against *Phytophthora* (Figure 6). This further confirms the role of IRE1/bZIP60 mediated UPR pathway in plant immunity. To the best of our knowledge, although bZIP28-mediated UPR pathway confers overlapping functions with IRE1–bZIP60 UPR pathway in fundamental biology (Liu et al., 2007; Gao et al., 2008), its function in response to biotic stress such as pathogen infection is largely unknown. Notably, we found that *bzip28* mutants resembled the susceptible phenotype of *bzip60* mutants in response to *P. parasitica* infection (Figure 6). This implies that bZIP28 UPR pathway may also function in plant immune response to microbial infection. More interestingly, our study further reveals that both bZIP60 and bZIP28 play a role in *RTP1*-mediated plant immunity, as demonstrated by the attenuated flg22-triggered oxidative burst (Figure 7B), reduced callose deposition upon infection (Figure 7, D and F) and compromised resistance against *P. parasitica* in mutants *rtp1bzip60* and *rtp1bzip28* compared with *rtp1* (Figure 6).

Notably, our finding that strong induction of expression of ER stress-responsive immune genes in *rtp1* mutants during the early infection is significantly attenuated in mutants *rtp1bzip60* and *rtp1bzip28* (Figure 7A; Supplemental Table S1) further indicates that the activation of these immune-related genes is regulated by bZIP60 and bZIP28 TFs. With analysis on the promoter regions of these genes through plantCARE (<http://bioinformatics.psb.ugent.be/webtools/plantcare/html/>), the CCAAT box, a key motif of ER stress response element-1 *cis*-element required for the interaction with bZIP TFs (Liu and Howell, 2010), is identified in the promoter regions of *WRKY33*, *CBP60g*, and *CYP71A12* (Supplemental Figure S10). Further studies are needed to understand the interaction of bZIP60 and bZIP28 TFs with the promoter of these ER stress-responsive immune genes

presented show means of three independent experiments \pm SE. Asterisks indicate significance at * P < 0.05 and ** P < 0.01 analyzed by Student's *t* test. B, ROS burst upon flg22 treatment of leaves of 4-week-old WT Col-0 as well as mutants *rtp1*, *bzip60*, *bzip28*, *rtp1bzip60*, and *rtp1bzip28*. At least 12 leaves from 6 plants of each group were measured using a luminol-based chemiluminescence assay. Data presented show means \pm SD (n = 12). Three independent experiments were repeated with similar results. RLU, relative light units. C–F, Leaves of 4-week-old WT Col-0 and *rtp1* plants were treated with 1 μ M flg22 for 24 h (C and E) and leaves of 4-week-old WT Col-0, *rtp1*, *rtp1bzip28*, and *rtp1bzip60* plants were inoculated by *P. parasitica* zoospores for 24 h (D and F). Leaves were fixed in ethanol–glacial acetic acid and stained by aniline blue for 2 h. Callose depositions were detected by fluorescence microscopy. Bar = 250 μ m (C and D). Callose deposits were quantified as the number of depositions per 4 mm² (E and F). Data presented show means \pm SE (n = 10). Asterisks denote significant differences analyzed by Student's *t* test (* P < 0.05, ** P < 0.01). Three independent experiments were repeated with similar results.

that are modulated by the susceptibility factor RTP1. Nevertheless, our results point to the notion that bZIP60 TF can possibly have functional overlapping with bZIP28 TF in *rpt1*-mediated plant resistance against *P. parasitica* through regulating the expression of downstream ER stress-responsive immune genes. This may explain why the intermediate susceptible phenotype of *rtp1bzp60* resembled that of *rtp1bzp28* (Figure 6, A and C), as the absent transcriptional activity of bZIP60 TF might be compensated by the bZIP28 TF in the *rtp1bzp60* mutant.

Collectively, we propose a mechanism to explain how plant susceptibility factor RTP1 negatively regulates resistance to biotrophic pathogens: RTP1 is involved in UPR regulation in response to *P. parasitica* infection, and may exert negative modulating roles in the activation of ER-localized UPR TFs bZIP60 and bZIP28, which are possibly shared to facilitate synergistic signaling between UPR and plant immunity (Figure 8).

Materials and methods

Plant materials, growth conditions, and plant inoculation

The *Arabidopsis* (*Arabidopsis thaliana*) RTP1 T-DNA insertion line (SALK_094320) was obtained from ABRC. The mutants of *bzp28*, *bzp60* and *vpe* (Qiang et al., 2012) were provided by Dr P. Schäfer. The double mutants of *rtp1bzp60* and *rtp1bzp28* were generated by crossing *rtp1* with *bzp60* and *bzp28*. The T-DNA insertion homozygous mutants were confirmed by PCR using primers *rtp1*-LP, *rtp1*-RP, *bzp28*-LP, *bzp28*-RP, *bzp60*-LP, *bzp60*-RP, and LbB1.3 (Supplemental Table S2). For root inoculation or chemical

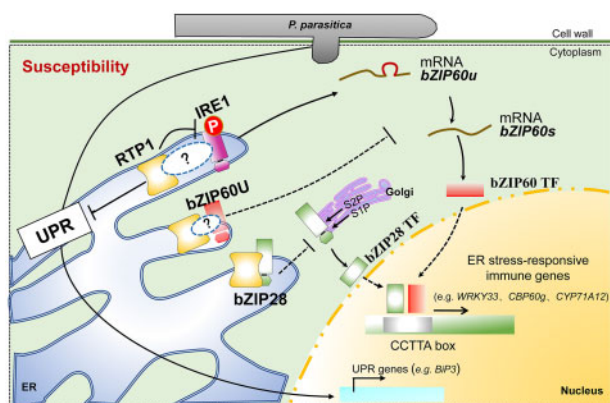


Figure 8 A schematic model of RTP1 negatively regulates plant immunity via modulating UPR TFs bZIP60 and bZIP28. We formerly demonstrated that *Arabidopsis* RTP1 is a plant susceptibility factor which negatively regulates resistance against biotrophic pathogens (Pan et al., 2016). Based on our data, RTP1 is involved in UPR regulation in response to *P. parasitica* infection, and contributes to stabilize the ER membrane-associated bZIP60 and bZIP28 stress sensors through manipulating IRE1-mediated bZIP60 splicing activity and interacting with bZIP28. The outcome of these events attenuates the activation of downstream UPR genes and ER stress-responsive immune genes regulated by activated forms of bZIP60 and bZIP28 TFs.

treatment, all *A. thaliana* seeds were sterilized and grown in squared petri dishes on half-strength Murashige and Skoog (MS). For leaf inoculation or treatment on leaves of *A. thaliana* and *N. benthamiana*, the plant growing conditions were as previously described (Pan et al., 2016). The culture and inoculation of *P. parasitica* strain Pp016, as well as the quantitation of *P. parasitica* infection by qPCR were conducted as previously described (Wang et al., 2011; Pan et al., 2016).

Plasmid constructs

For the creation of firefly luciferase complementation constructs, the coding regions of RTP1, bZIP28, BI-1, IRE1a, and IRE1b were cloned from *A. thaliana* WT Col-0 cDNA and inserted into the *Kpn1* and *Sal1* site of pCAMBIA1300 (Chen et al., 2008). The sequence of RTP1 was fused upstream of N-Luc in the pCAMBIA-NLuc vector, and bZIP28, BI-1, IRE1a, and IRE1b were fused downstream of C-Luc in the pCAMBIA-CLuc vector. To create 7×myc-fusion plasmids, the 7×myc fragment was cloned into pKannibal (Wesley et al., 2001) with *Xho1* and *EcoR1* sites and *Not1* sites were used to release the fragment with the promoter and terminator and then inserted into the binary vector pART27 (Gleave, 1992). The mature bZIP28, bZIP60, IRE1a, and IRE1b coding sequences were inserted into previously modified pART27 at the *EcoR1* and *Xba1* sites to create 7×myc-bZIP28, 7×myc-bZIP60, 7×myc-IRE1a, and 7×myc-IRE1b. For other plant expression constructs, including RTP1-FLAG and FLAG-GFP, fusion fragments were obtained from overlapping PCR and cloned into the *EcoR1* and *Xba1* sites of the previously described plant expression vector, replacing the existing sequence.

For the creation of phosphorylation assay constructs, the fusion fragments IRE1a-3×Flag, SP-3×Flag-IRE1b.1, IRE1b.1-3×Flag, and RTP1-HA were obtained through overlapping PCR and inserted into the monoclonal site of pKannibal (IRE1a-3×Flag: *Xho1* and *BamHI*; SP-3×Flag-IRE1b.1 and IRE1b.1-3×Flag: *Xho1* and *HindIII*; RTP1-HA: *EcoR1* and *Xba1*), and thereafter inserted into the binary vector pART27 at the *Not1* site.

Plant recovery and growth retardation assays

Seeds were sterilized and treated by TM (0.3 μg/mL) or DTT (2 mM) as previously described (Moreno et al., 2012). After TM or DTT exposure, 30 seeds per line were transferred to 1/2 MS 0.8% (w/v) agar medium supplemented with ampicillin (50 μg/mL), and grown in a horizontal direction. After 10 d growth, survival seedlings were recorded. Percentage of recovery was calculated as described (Moreno et al., 2012). For growth retardation assay, 5-d-old *A. thaliana* seedlings grown in 1/2MS medium were transferred into 1/2 MS + 1% sucrose (w/v) liquid medium with TM (75 ng/mL)/DTT (2 mM) or DMSO (control), respectively. These seedlings were placed in 96-well plates. At least 10 plants per line were treated. The seedlings fresh weight was measured at 5 d after treatment. Relative fresh weight was plotted by calculating treatment/control seedlings.

Gene expression analysis

Total RNA was extracted from root material by using TRIzol (Invitrogen) reagent. For RT-qPCR analysis, cDNA was synthesized from 1 µg of total RNA using PrimeScript RT reagent Kit (TaKaRa). Twenty nanograms of cDNA were used as template for the amplification of candidate genes using SYBR premix Kit (Roche) according to the manufacturers' instructions. The primers we used are listed in [Supplemental Table S2](#). The Ct values of genes were quantified using an iQ7 Real-Time Cycler (Life technologies, USA). Expression fold changes were calculated by the $2^{-\Delta\Delta Ct}$ method ([Schmittgen and Livak, 2008](#)).

For RT-qPCR-based bZIP60 splicing assay, cDNA was used as template. The bZIP60 splicing activity was analyzed as described ([Moreno et al., 2012](#)).

Firefly luciferase complementation imaging assay

The constructed vectors were transformed into *Agrobacterium* strain GV3101 and then infiltrated *N. benthamiana* leaves. After 3 d, 1 mM beetle luciferin (Promega) was sprayed on leaves and kept dark for 6 min at room temperature to quench the autofluorescence. A low-light cooled charge-coupled device camera (Lumazone Pylon 2048B, Princeton, USA) was used to capture the LUC image. The camera was cooled at -120°C and used to measure the relative LUC activity as described ([Chen et al., 2008](#)).

Co-IP and immunoblot assays

Nicotiana benthamiana leaves were harvested at indicated timepoints after agroinfiltration and proteins were extracted with a buffer containing 250 mM sucrose, 50 mM HEPES-KOH, 5% glycerin, 1 mM $\text{Na}_2\text{MoO}_4 \times 2 \text{H}_2\text{O}$, 25 mM NaF, and 10 mM EDTA. Co-IP was performed as described ([Win et al., 2011](#)). Precipitates by anti-FLAG M2 affinity gel (Sigma-Aldrich) or anti-Myc magnetic beads (Bimake) were washed at least five times with GTEN buffer (10% glycerol, 25 mM Tris [pH 7.5], 1 mM EDTA, 150 mM NaCl) supplemented with 1 mM DTT and 0.15% NP40 (w/v; Sigma). Fusion proteins from crude extracts (input) and precipitated proteins were detected by IB with protein-specific antibodies. For immunodetection of BiP, Arabidopsis root extracts were separated by SDS-PAGE followed by transfer to polyvinylidene difluoride (PVDF) membranes (Roche). The polyclonal antibody anti-BiP2 (Agrisera, Sweden; AS09481) was used at a 1:5,000 dilution and followed by incubation with a second antibody, anti-rabbit Ig-horseradish peroxidase (#AS014, ABclonal). Protein bands were quantified using Image J software ([Schneider et al., 2012](#)).

Phosphorylation assay

The constructs of *IRE1a-3×FLAG* and *RTP1-HA*, *3×FLAG-IRE1b*, and *RTP1-HA*, *IRE1a-3×FLAG* and *EV*, *3×FLAG-IRE1b* and *EV*, were cotransformed using the *Agrobacterium*-mediated transient transformation in leaves of 6-week-old *N. benthamiana*. At 3 d post coinfiltration, the leaves were harvested and total proteins were extracted using HEPES buffer containing phosphatase inhibitor cocktail (Sigma)

1:100. The Phos-tag indicator (#300-93523, Wako) and MnCl_2 were used to distinguish the phosphorylated and non-phosphorylated proteins ([Kaps et al., 2015](#)). After SDS-PAGE, the gel was soaked in a transfer buffer containing 10 mM EDTA and gently incubated for 10 min for three times, and then soaked in a transfer buffer without EDTA and gently shaken for 10 min. The accumulation of phosphorylated and nonphosphorylated proteins was analyzed by IB using protein-specific antibodies. The band intensities of phosphorylated and unphosphorylated IRE1 proteins were determined by the gray values using Image J. In order to compare intensities of IRE1 phosphorylation in different samples in parallel, the band intensities of unphosphorylated IRE1 proteins in control samples (i.e. *IRE1a-FLAG* or *FLAG-IRE1b + EV*) were used as the calibrator; whereas the band intensities of phosphorylated IRE1 proteins in the tested samples (i.e. *IRE1a-FLAG* or *FLAG-IRE1b + RTP1-HA*) were calculated by an adjusted factor calculated as follows:

$$\text{Adjusted factor} = \frac{\text{intensity of UP (negative control)}}{\text{intensity of UP (tested sample)}}$$

$$\text{Adjusted intensity} = \text{intensity of P (tested sample)} \times \text{adjusted factor}$$

(UP, unphosphorylated IRE1; P, phosphorylated IRE1)

The adjusted band intensities of phosphorylated IRE1 proteins in the tested samples were normalized with the band intensities of phosphorylated IRE1 proteins in control samples, which were set to 1.

Callose deposition assay

The callose assay was performed as described ([Luna et al., 2011](#)). Briefly, the 4-week-old *A. thaliana* plant leaves were infiltrated with 1 µM flg22 for 24 h or infected by *P. parasitica* zoospores for 24 h. Leaves were cut, fixed, and destained in ethanol:glacial acetic acid (3:1, v/v) with 1× change of the solution until the leaves were transparent. Thereafter, leaves were rehydrated in 70% ethanol for 15 min, and then in 50% ethanol for 15 min. After several washes with water, leaves were incubated for 2 h in 150 mM K_2HPO_4 (pH 9.5) solution containing 0.01% aniline blue (w/v) in darkness. Callose deposits were detected using Olympus BX63 microscope (excitation, 365 nm; emission, 420 nm) and quantitated from digital photographs with Image J software ([Schneider et al., 2012](#)).

Oxidative burst assay

ROS production was measured with a previously reported luminol-based assay ([Sang and Macho, 2017](#)). The leaf disks 5 mm in diameter were cut from the 7-week-old *A. thaliana* plant leaves with sharp puncher and were floated in 200 µL H_2O overnight. Water was replaced with reagent containing luminol, peroxidase, and 1 µM flg22. ROS released by leaf discs was detected by luminescence of luminol. Luminescence was measured at 535 nm (excitation 490 nm) in a TECAN Infinite F200 microplate reader (TECAN, Switzerland).

Agroinfiltration and confocal laser scanning microscopy

Agrobacterium tumefaciens strain GV3101 cells transformed with individual vector constructs were grown in Luria–Bertani medium with appropriate antibiotics at 28°C for about 36 h. Agrobacteria were pelleted, resuspended in infiltration buffer (10 mM MES, 10 mM MgCl₂, and 200 mM acetosyringone) and adjusted to the required concentration (OD₆₀₀ 0.3) before being infiltrated into the 4- to 6-week-old *N. benthamiana* leaves.

Nicotiana benthamiana cells expressing fusion proteins were observed 2 or 3 d after infiltration using an Olympus FV3000 confocal microscope (Japan). GFP was detected after excitation with a 488 nm wavelength laser, and emissions were collected at 500–540 nm. The fluorescence of mCherry was excited with a 559 nm wavelength laser to detect specific emissions at 600–680 nm.

Statistical analysis

Results are expressed as means \pm standard deviation (SD) or \pm standard error (SE) as indicated in the figure legends and represent at least three biological repetitions. Statistical analysis was performed using Student's *t* test. *P* < 0.05 was considered to be significant.

Accession numbers

Sequence data from this article can be found in the Arabidopsis Genome Initiative or GenBank/EMBL database under the following accession numbers: *Arabidopsis*: RTP1 (AT1G70260), bZIP60 (AT1G42990), IRE1a (AT2G17520), IRE1b (AT5G24360), bZIP28 (AT3G10800), BiP3 (AT1G09080), DnaJ (AT1G56300), WRKY33 (AT2G38470), WRKY46 (AT2G46400), CBP60g (AT5G26920), CYP71A12 (AT2G30750) and MPK11 (AT1G01560).

Supplemental data

The following materials are available in the online version of this article.

Supplemental Figure S1. Analysis on the protein stability of myc-GFP in the presence of RTP1.

Supplemental Figure S2. RTP1 colocalizes with bZIP60 in the ER membrane.

Supplemental Figure S3. Independent analysis on the phosphorylation of IRE1 protein.

Supplemental Figure S4. RTP1 attenuates the protein stability of IRE1 protein.

Supplemental Figure S5. Analysis on protein interaction between RTP1 and IRE1.

Supplemental Figure S6. Co-immunoprecipitation assay on protein interaction between RTP1 and bZIP28.

Supplemental Figure S7. *EFR* and γ VPE show increased expressions in *P. parasitica*-infected *rtp1* mutants.

Supplemental Figure S8. RTP1 colocalizes with bZIP28 in the ER membrane.

Supplemental Figure S9. Analysis on protein interaction between RTP1 and BI-1.

Supplemental Figure S10. Diagrams showing regulatory elements in the promoter regions of immune genes *WRKY33*, *CBP60g*, and *CYP71A12*.

Supplemental Table S1. Immune genes induced more than four-fold by tunicamycin treatment in *A. thaliana* WT Col-0 plants.

Supplemental Table S2. List of primers used in this study.

Acknowledgments

We thank Dr Jim Peacock and Dr Liz Dennis (CSIRO Agriculture, Canberra, Australia); Dr Brett Tyler (Oregon State University, USA); Dr Patrick Schäfer and Dr Ruth Schäfer (The University of Warwick, UK); and Dr Qiaojun Jin (Northwest A&F University, China) for discussions and their insightful suggestions; Dr Fei Zhang for technical support in Firefly Luciferase Complementation Imaging Assay and infection assay; Ms Zhenzhen Ma and Dr Hua Zhao for technical support in confocal microscopy analysis; Dr Yi Li (Peking University, China) for providing pCAMBIA1300-nLUC and pCAMBIA1300-cLUC constructs; and Dr Patrick Schäfer for providing mutants of *bzip28*, *bzip60*, and γ vpe.

Funding

The work was funded by National Natural Science Foundation of China (#31872657 and #31125022), National Key R&D Program of China (#2017YFD0200602-2), China Agriculture Research System (#CARS-09), and Program of Introducing Talents of Innovative Discipline to Universities (Project 111) from the State Administration of Foreign Experts Affairs (#B18042).

Conflict of interest statement. The authors declare no conflict of interest.

References

- Chen HM, Zou Y, Shang YL, Lin HQ, Wang YJ, Cai R, Tang XY, Zhou JM (2008) Firefly luciferase complementation imaging assay for protein-protein interactions in plants. *Plant Physiol* **146**: 368–376
- Deng Y, Humbert S, Liu JX, Srivastava R, Rothstein SJ, Howell SH (2011) Heat induces the splicing by IRE1 of a mRNA encoding a transcription factor involved in the unfolded protein response in Arabidopsis. *Proc Natl Acad Sci USA* **108**: 7247–7252
- Deng Y, Srivastava R, Howell SH (2013) Protein kinase and ribonuclease domains of IRE1 confer stress tolerance, vegetative growth, and reproductive development in Arabidopsis. *Proc Natl Acad Sci USA* **110**: 19633–19638
- Dodds PN, Rathjen JP (2010) Plant immunity: towards an integrated view of plant-pathogen interactions. *Nat Rev Genet* **11**: 539–548
- Fan GJ, Yang Y, Li TT, Lu WQ, Du Y, Qiang XY, Wen QJ, Shan WX (2018) A *Phytophthora capsici* RXLR effector targets and inhibits a plant PPLase to suppress endoplasmic reticulum-mediated immunity. *Mol Plant* **11**: 1067–1083
- Fry W (2008) *Phytophthora infestans*: the plant (and R gene) destroyer. *Mol Plant Pathol* **9**: 385–402
- Gao H, Brandizzi F, Benning C, Larkin RM (2008) A membrane-tethered transcription factor defines a branch of the heat stress response in *Arabidopsis thaliana*. *Proc Natl Acad Sci USA* **105**: 16398–16403

- Glazebrook J** (2005) Contrasting mechanisms of defense against biotrophic and necrotrophic pathogens. *Annu Rev Phytopathol* **43**: 205–227
- Gleave AP** (1992) A versatile binary vector system with a T-DNA organizational structure conducive to efficient integration of cloned DNA into the plant genome. *Plant Mol Biol* **20**: 1203–1207
- Hayashi S, Wakasa Y, Takaiwa F** (2012) Functional integration between defense and IRE1-mediated ER stress response in rice. *Sci Rep* **2**: 670
- Howell SH** (2013) Endoplasmic reticulum stress responses in plants. *Annu Rev Plant Biol* **64**: 477–499
- Humbert S, Zhong S, Deng Y, Howell SH, Rothstein SJ** (2012) Alteration of the bZIP60/IRE1 pathway affects plant response to ER stress in *Arabidopsis thaliana*. *PLoS One* **7**: e39023
- Hu Y, Dong Q, Yu D** (2012). *Arabidopsis WRKY46* coordinates with *WRKY70* and *WRKY53* in basal resistance against pathogen *Pseudomonas syringae*. *Plant Sci* **185**: 288–297
- Iwata Y, Ashida M, Hasegawa C, Tabara K, Mishiba K, Koizumi N** (2017) Activation of the *Arabidopsis* membrane-bound transcription factor bZIP28 is mediated by site-2 protease, but not site-1 protease. *Plant J* **91**: 408–415
- Iwata Y, Fedoroff NV, Koizumi N** (2008) *Arabidopsis* bZIP60 is a proteolysis-activated transcription factor involved in the endoplasmic reticulum stress response. *Plant Cell* **20**: 3107–3121
- Iwata Y, Koizumi N** (2005) An *Arabidopsis* transcription factor, AtbZIP60, regulates the endoplasmic reticulum stress response in a manner unique to plants. *Proc Natl Acad Sci USA* **102**: 5280–5285
- Iwata Y, Koizumi N** (2012) Plant transducers of the endoplasmic reticulum unfolded protein response. *Trend Plant Sci* **17**: 720–727
- Jäger R, Bertrand MJ, Gorman AM, Vandenabeele P, Samali A** (2012) The unfolded protein response at the cross roads of cellular life and death during endoplasmic reticulum stress. *Biol Cell* **104**: 259–270
- Jones JD, Dangl JL** (2006) The plant immune system. *Nature* **444**: 323–329
- Kaps S, Kettner K, Migotti R, Kanashova T, Krause U, Rödel G, Dittmar G, Kriegel TM** (2015) Protein kinase Ymr291w/Tda1 is essential for glucose signaling in *Saccharomyces cerevisiae* on the level of hexokinase isoenzyme ScHxk2 phosphorylation. *J Biol Chem* **290**: 6243–6255
- Kinoshita E, Kinoshita-Kikuta E, Takiyama K, Koike T** (2006) Phosphate-binding tag, a new tool to visualize phosphorylated proteins. *Mol Cell Proteom* **5**: 749–757
- Koizumi N, Martinez, IM, Kimata, Y, Kohno K, Sano H, Chrispeels MJ** (2001) Molecular characterization of two *Arabidopsis* Ire1 homologs, endoplasmic reticulum-located transmembrane protein kinases. *Plant Physiol* **127**: 949–962
- Körner CJ, Du X, Vollmer ME, Pajeroska-Mukhtar KM** (2015) Endoplasmic reticulum stress signaling in plant immunity—at the crossroad of life and death. *Int J Mol Sci* **16**: 26582–26598
- Lacombe S, Rougon-Cardoso A, Sherwood E, Peeters N, Dahlbeck D, van Esse HP, Smoker M, Rallapalli G, Thomma BP, Staskawicz B, et al.** (2010) Interfamily transfer of a plant pattern-recognition receptor confers broad-spectrum bacterial resistance. *Nat. Biotechnol* **28**: 365–369
- Lai YS, Renna L, Yarema J, Ruberti C, He SY, Brandizzi F** (2018) Salicylic acid-independent role of NPR1 is required for protection from proteotoxic stress in the plant endoplasmic reticulum. *Proc Natl Acad Sci USA* **115**: 5203–5212
- Li J, Zhao-Hui C, Batoux M, Nekrasov V, Roux M, Chinchilla D, Zipfel C, Jones JD** (2009) Specific ER quality control components required for biogenesis of the plant innate immune receptor EFR. *Proc Natl Acad Sci USA* **106**: 15973–15978
- Li W, Zhu Z, Chern M, Yin J, Yang C, Ran L, Cheng M, He M, Wang K, Wang J, et al.** (2017) A natural allele of a transcription factor in rice confers broad-spectrum blast resistance. *Cell* **170**: 114–126
- Li Y, Williams B, Dickman M** (2017) *Arabidopsis* B-cell lymphoma2 (Bcl-2)-associated athanogene 7 (BAG7)-mediated heat tolerance requires translocation, sumoylation and binding to WRKY29. *New Phytol* **214**: 695–705
- Lisbona F, Rojas-Rivera D, Thielen P, Zamorano S, Todd D, Martinon F, Glavic A, Kress C, Lin JH, Walter P, et al.** (2009) BAX inhibitor-1 is a negative regulator of the ER stress sensor IRE1alpha. *Mol Cell* **33**: 679–691
- Liu JX, Howell SH** (2010) Endoplasmic reticulum protein quality control and its relationship to environmental stress responses in plants. *Plant Cell* **22**: 2930–2942
- Liu JX, Howell SH** (2016) Managing the protein folding demands in the endoplasmic reticulum of plants. *New Phytol* **211**: 418–428
- Liu JX, Srivastava R, Che P, Howell SH** (2007) An endoplasmic reticulum stress response in *Arabidopsis* is mediated by proteolytic processing and nuclear relocation of a membrane-associated transcription factor, bZIP28. *Plant Cell* **19**: 4111–4119
- Luna E, Pastor V, Robert J, Flors V, Mauch-Mani B, Ton J** (2011) Callose deposition: a multifaceted plant defense response. *Mol Plant Microbe Interact* **24**: 183–193
- Meng Y, Zhang Q, Ding W, Shan W** (2014) *Phytophthora parasitica*: a model oomycete plant pathogen. *Mycology* **5**: 43–51
- Millet YA, Danna CH, Clay NK, Songnuan W, Simon MD, Werck-Reichhart D, Ausubel FM** (2010) Innate immune responses activated in *Arabidopsis* roots by microbe-associated molecular patterns. *Plant Cell* **22**: 973–990
- Mishiba K, Nagashima Y, Suzuki E, Hayashi N, Ogata Y, Shimada Y, Koizumi N** (2013) Defects in IRE1 enhance cell death and fail to degrade mRNAs encoding secretory pathway proteins in the *Arabidopsis* unfolded protein response. *Proc Natl Acad Sci USA* **110**: 5713–5718
- Moreno, AA, Mukhtar, MS, Blanco F, Boatwright JL, Moreno I, Jordan MR, Chen Y, Brandizzi F, Dong X, Orellana A, et al.** (2012). IRE1/bZIP60-mediated unfolded protein response plays distinct roles in plant immunity and abiotic stress responses. *PLoS One* **7**: e31944
- Nagashima Y, Mishiba K, Suzuki E, Shimada Y, Iwata Y, Koizumi N** (2011) *Arabidopsis* IRE1 catalyses unconventional splicing of bZIP60 mRNA to produce the active transcription factor. *Sci Rep* **1**: 29
- Nekrasov V, Li J, Batoux M, Roux M, Chu ZH, Lacombe S, Rougon A, Bittel P, Kiss-Papp M, Chinchilla D, et al.** (2009) Control of the pattern-recognition receptor EFR by an ER protein complex in plant immunity. *EMBO J* **28**: 3428–3438
- Pan Q, Cui B, Deng F, Quan J, Loake GJ, Shan W** (2016) *RTP1* encodes a novel endoplasmic reticulum (ER)-localized protein in *Arabidopsis* and negatively regulates resistance against biotrophic pathogens. *New Phytol* **209**: 1641–1654
- Pavan S, Jacobsen E, Visser RGF, Bai YL** (2010) Loss of susceptibility as a novel breeding strategy for durable and broad-spectrum resistance. *Mol Breed* **25**: 1–12
- Qiang X, Zechmann B, Reitz MU, Kogel KH, Schäfer P** (2012) The mutualistic fungus *Piriformospora indica* colonizes *Arabidopsis* roots by inducing an endoplasmic reticulum stress-triggered caspase-dependent cell death. *Plant Cell* **24**: 794–809
- Ruberti C, Kim SJ, Stefano G, Brandizzi F** (2015) Unfolded protein response in plants: one master, many questions. *Curr Opin Plant Biol* **27**: 59–66
- Saijo Y, Tintor N, Lu X, Rauf P, Pajeroska-Mukhtar K, Häweker H, Dong X, Robatzek S, Schulze-Lefert P** (2009) Receptor quality control in the endoplasmic reticulum for plant innate immunity. *EMBO J* **28**: 3439–3449
- Sang Y, Macho AP** (2017) Analysis of PAMP-triggered ROS burst in plant immunity. *Methods Mol Biol* **1578**: 143–153
- Schmittgen TD, Livak KJ** (2008) Analyzing real-time PCR data by the comparative C(T) method. *Nat Protoc* **3**: 1101–1108
- Schneider CA, Rasband WS, Eliceiri KW** (2012) NIH Image to ImageJ: 25 years of image analysis. *Nat Method* **9**: 671–675

- Srivastava R, Chen Y, Deng Y, Brandizzi F, Howell SH** (2012) Elements proximal to and within the transmembrane domain mediate the organelle-to-organelle movement of bZIP28 under ER stress conditions. *Plant J* **70**: 1033–1042
- Tateda C, Ozaki R, Yu O, Takahashi Y, Yamaguchi K, Berberich T, Koizumi N, Kusano T** (2008) NtbZIP60, an endoplasmic reticulum-localized transcription factor, plays a role in the defense response against bacterial pathogens in *Nicotiana tabacum*. *J Plant Res* **121**: 603–611
- Tsuda K, Sato M, Stoddard T, Glazebrook J, Katagiri F** (2009) Network properties of robust immunity in plants. *PLoS Genet* **5**: e1000772
- Truman W, Glazebrook J** (2012) Co-expression analysis identifies putative targets for CBP60g and SARD1 regulation. *BMC Plant Biol* **12**: 216
- van Schie CC, Takken FL** (2014) Susceptibility genes 101: how to be a good host. *Annu Rev Phytopathol* **52**: 551–581
- Wakasa Y, Oono Y, Yazawa T, Hayashi S, Ozawa K, Handa H, Matsumoto T, Takaiwa F** (2014) RNA sequencing-mediated transcriptome analysis of rice plants in endoplasmic reticulum stress conditions. *BMC Plant Biol* **14**: 101
- Wang D, Weaver ND, Keserwani M, Dong X** (2005) Induction of protein secretory pathway is required for systemic acquired resistance. *Science* **308**: 1036–1040
- Wang Y, Meng Y, Zhang M, Tong X, Wang Q, Sun Y, Quan J, Govers F, Shan W** (2011) Infection of *Arabidopsis thaliana* by *Phytophthora parasitica* and identification of variation in host specificity. *Mol Plant Pathol* **12**: 187–201
- Wesley SV, Helliwell CA, Smith NA, Wang M, Rouse DT, Liu Q, Gooding PS, Singh SP, Abbott D, Stoutjesdijk PA, et al.** (2001) Construct design for efficient, effective and high-throughput gene silencing in plants. *Plant J* **27**: 581–590
- Williams B, Kabbage M, Britt R, Dickman MB** (2010) AtBAG7, an Arabidopsis Bcl-2-associated athanogene, resides in the endoplasmic reticulum and is involved in the unfolded protein response. *Proc Natl Acad Sci USA* **107**: 6088–6093
- Win J, Kamoun S, Jones AE** (2011) Purification of effector target protein complexes via transient expression in *Nicotiana benthamiana*. *Method Mol Biol* **712**: 181–194
- Zhang L, Chen H, Brandizzi F, Verchot J, Wang A** (2015) The UPR branch IRE1-bZIP60 in plants plays an essential role in viral infection and is complementary to the only UPR pathway in yeast. *PLoS Genet*. **11**: e1005164
- Zhang L, Zhang C, Wang A** (2016) Divergence and conservation of the major UPR branch IRE1-bZIP signaling pathway across eukaryotes. *Sci Rep* **6**: 27362.